
CEDAR2019



Eldorado Hotel
Santa Fe, New Mexico

IT Studies Poster Session
Wednesday June 19, 2019

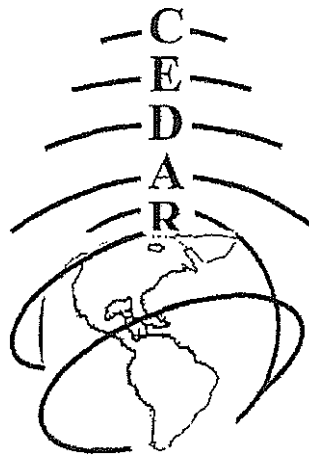


Table of Contents

Irregularities of Ionosphere or Atmosphere

IRRI-01	Valerie Bernstein, Investigating Atmospheric Drag Coefficient Composition Sensitivities.....	1
IRRI-02	Cheng Ming Hong, Characteristics of ES and Flayer observed by CODAR SeaSonde HF radar.....	1-2
IRRI-03	Shih-Ping Chen, Global scintillation occurrence calculated by FORMOSAT - 3/COSMIC S4-index-.....	2
IRRI-04	Thomas Coppeans, GNSS TEC and Scintillation Variations Following Solar Wind Dynamic Pressure Enhancement.....	2
IRRI-05	Lindsay Goodwin, The role of substorms in polar cap formation.....	3
IRRI-06	John Elliott, Observations of Spatiotemporally local Structure in the Thermosphere over Alaska.....	3
IRRI-07	Wendell Horton, Auroral beads first stage of Substorm Onset.....	3
IRRI-08	Jonathon Smith, Equatorial Plasma Bubble Growth: Preliminary Numerical Assessment	4
IRRI-09	Leslie Lamarche, Analysis of plasma irregularities on a range of scintillation-scales using the Resolute Bay Incoherent Scatter Radars.....	4
IRRI-10	Robert Irvin, A study of Polar Cap Patches using RISR	4
IRRI-11	Matthew Young, The Farley-Buneman Spectrum in 2-D and 3-D PIC Simulations	5
IRRI-12	Jiaen Ren, Multi-scale Observations of High-Latitude Ionosphere Plasma Transport During Oct. 12, 2016 Geomagnetic Storm.....	5
IRRI-13	Zhe Yang, A Global View of Ionospheric Response Impacts on Kinematic GPS Positioning during the 2015 St Patrick's Day Storm.....	6
IRRI-14	Pralay Raj Vaggu, A case study to understand the ionospheric structures over Poker Flat Research Range using forward propagation model SIGMA and Configuration Space Model	6-7

IRRI-15	Weijia Zhan, MELISSA studies of equatorial spread F: Post-midnight events	7
IRRI-16	Dallin Smith, FDTD Modeling of HF Waves Through Ionospheric Plasma Irregularities	7
IRRI-17	Aurora Lopez, Overview of scintillation events due to E region and F region as inferred from SAGA	8
IRRI-18	Sebastijan Mrak, Multi-scale density irregularities at mid-latitudes: GPS scintillation imaging	8
IRRI-19	Enrique Rojas Villalba, Hybrid Simulations of Farley Buneman Instabilities in the Auroral E Region	9
IRRI-20	Anahita Shahbazi, An effective technique for isolation of Traveling Ionospheric Disturbances from GNSS-derived Total Electron Content measurements	9-10
IRRI-21	Jack Wang, ROT! estimation by dual-frequency GPS receiver measurements during magnetic storms	10
IRRI-22	Dev Joshi, Peak Height Distributions of Equatorial Ionospheric Irregularities deduced from the C/NOFS satellite mission	10

Instruments or Techniques for Ionospheric or Thermospheric Observation

ITIT-01	Augustine Yellu, Observations of Second Harmonic Generation in Stimulated Electromagnetic Emissions during Ionospheric Heating	11
ITIT-02	Chi-Ting Liao, Performance Assessment and Improvements for the FORMOSAT-5 Onboard Orbit Propagator Using GPS Ephemeris	11-12
ITIT-03	Cesar De La Jara, Ionospheric Echoes Detection in Digital Ionograms Using Convolutional Neural.....	12
ITIT-04	Brian Breitsch, False Detection of Ionosphere-Induced GNSS Cycle Slips at High- Latitude	12-13
ITIT-05	William Longley, Electron collision effects on ISR temperature measurements of the ionosphere	13
ITIT-06	Meghan LeMay, Northern Alaska Receiver Comparison	14
ITIT-07	Joseph Malins, Three Dimensional Mapping of Lightning Produced Ionospheric Reflections.....	14
ITIT-08	Himani Dewan, Terahertz emission by the nonlinear coupling of Laser and Kinetic Alfvén wave in a magnetized plasma	14

ITIT-09	Benjamin Obom, Gridded Retarding Ion Drift Sensor (GRIDS) for PetitSat.....	15
ITIT-10	Kai-Jun Ke, - Using two dimensional autocorrelation method to improve the performance of automatic algorithm on ionogram.....	15
ITIT-11	Alex Hoffinan, Daedalus: ESA's Earth Explorer 10 mission candidate for thermosphere-ionosphere studies.....	15-16
ITIT-12	Narender Kumar, Ion acoustic terahertz generation by a femtosecond laser pulse in plasma	16
ITIT-13	Hassan Akbari, In-situ electron density from Langmuir waves: the influence of the spacecraft wake.....	16-17
ITIT-14	Victoriya Forsythe, Comparison of Ionospheric Electron Density Retrieved from Spire Global Radio Occultation Data with Arecibo Incoherent Scatter Radar and Ionosonde Measurements	17
ITIT-15	Scott Palo, Space Weather Atmospheric Reconfigurable Multiscale Experiment Cubesat	17-18
ITIT-16	Piyush Mehta, On Deriving Self-consistent, High-accuracy Mass Density Measurements	18
ITIT-17	ZhiQing Chen, The Chinese Meridian Project for Space Weather Monitoring....	18

MidLatitude Thermosphere or Ionosphere

MDIT-01	Shantaqnaab Debchoudhury, A Machine Learning-based study of TEC variations in response to large equinoctial geomagnetic storms	19
MDIT-02	Shibaji Chala-aborty, A Study of Solar Flare Effects on Mid and High Latitude Radio Wave Propagation using SuperDARN	19
MDIT-03	Daniel Weimer, A High-Resolution Model of Exospheric Temperatures	20
MDIT-04	Brandon Ponder, Solving for the Thermal Conductivity Coefficients Experimentally	20
MDIT-05	Justin Yonker, Retrieval of Thermospheric Atomic Nitrogen using Preassociative Nitric Oxide Delta Band Emissions	20-21
MDIT-06	Pratik Joshi, Parametric estimation of neutral hydrogen density using proton continuity balance with TIMED/GUY! and SAMI3.....	21
MDIT-07	Olusegun Jonah, - Source Investigation and analysis of TIDs over equatorial and low-latitude regions.....	21-22

MDIT-08	Olusegun Jonah, - Dynamic response of ionospheric plasma density to the geomagnetic storm of 22-23 June 2015	22
MDIT-09	Lei Liu, Ionosphere responses to the May 2017 magnetic storm: Results from multi-instrumental observations over the Chinese sector.....	22
MDIT-10	Leonard Thomas, Comparative testing of electron density assimilative models.....	23

Magnetosphere - Ionosphere - Thermosphere Coupling

MITC-01	Crystal Moser, CAPER-2 and TRICE-2 Sounding Rocket Investigations: Wave-Particle and Wave-Wave Interactions in the Polar Cusp.....	23
MITC-02	Liam Kilcommons, Poynting Flux from DMSP in Auroral Boundary Coordinates.....	23-24
MITC-03	Robert Albarran, Kinetic modeling of auroral ion outflows	24
MITC-04	Kausik Chatterjee, A Hydrodynamic Model for Plasmasphere Refilling Following Geomagnetic Storms - by Kausik Chatterjee.....	24-25
MITC-05	Matthew Blandin, Time History Observations of Barium Releases from the C-REX Mission and their Relevance to the Ionosphere CUSP Region Density Anomaly	25
MITC-06	Yun-Ju Chen, Characteristics of meso-scale structures in the high-latitude ionosphere.....	25-26
MITC-07	Joaquin Diaz Pena, Small-scale convection cells in the polar ionosphere: Origins and implications for energy dissipation	26
MITC-08	Bharat Kunduri, An examination of inner-magnetosphere shielding by Region-2 Field-Aligned Currents.....	26-27
MITC-09	Benjamin Hogan, Alfvénic heating as a source of thermospheric density anomalies.....	27
MITC-10	Solene Lejosne, Electric Drift Morphology According to Van Allen Probes Measurements.....	27
MITC-11	Jun Liang, Determine the role of nitrogen ions in the ionospheric outflow	28

	Zhonghua Xu, A comparison of the ground magnetic responses during the 2013 and 2015 St. Patrick's Day geomagnetic storms	28
MITC-12		
	Yining Shi, Hemispheric Asymmetries in High-latitude Field-aligned Currents (FACs) Revealed by Inverse and Assimilative Analysis of AMPERE Magnetometer Data	29
MITC-13		
	Naomi Maruyama, On the factors that control plasmaspheric ion composition..	29
MITC-14		
	Haonan Wu, Localized Neutral Temperature Responses to Magnetosphere-Ionosphere-Thennosphere Coupling - A Mechanism Study of Temperature Inversion Layer	30
MITC-15		
	Astrid Maute, Simulating magnetosphere-ionosphere coupling via field- ligned current	30
MITC-16		
	Qingyu Zhu, Impacts of binning methods on high-latitude electrodynamic: Static vs boundary-oriented binning	31
MITC-17		
	Dogacan Ozturk, A case study of meso-scale electric fields and their effects on the I-T system	31
MITC-18		
	Nithin Sivadas, Optical Signature of Outer Radiation Belt Boundary	32
MITC-19		
	Boyi Wang, Ionosphere modulation by Pc5 ULF waves and wave structure detected by PFISR - by Boyi Wang	32
MITC-20		
	Zihan Wang, Storm-Enhanced Density (SED) Formation and Structuring During the September 7, 2017 Geomagnetic Storm - by Zihan Wang	33
MITC-21		
	Ying Zou, Effects of storms on high-latitude upper thermospheric winds.....	33
MITC-22		

Polar Aeronomy

POLA-01	Nathaniel Frissell, - Measuring Ionospheric Variability Using HF Signals of Opportunity in the Antarctic - by Nathaniel Frissell.	34
POLA-02	Kylee Branning, Comparison between 1-D and 4-D Ground Based Height Profiling Techniques to Resolve Altitude Variations of Neutral Winds in the Lower Thermosphere	34
POLA-03	Bruce Fritz, - UV Tomography in the Cusp	35

POLA-04	Carl Kjellstrand, High resolution Kelvin-Helmholtz Instabilities observed during the 2018 PMC Turbo flight	35
POLA-05	Andrew Kiene, The effect of sustained magnetic activity on Joule heating rates in the polar cap.....	36
POLA-06	Rajan Itani, Characterizing unexpected slowing of the Cross Polar Jet over Alaska in the midnight sector.....	36
POLA-07	Cissi Lin, Effects of Energetic Particle Precipitations on Thermospheric Nitric Oxide Cooling	37
POLA-08	Pablo Reyes, Overview of PFISR D-region capabilities	37
POLA-09	Qian Wu, New HIWIND Obsevational Results from 2018 Flight.....	38

CEDAR Workshop- IT Studies Session Abstracts

Day 2 - Wednesday, June 19, 2019

IRRI01- Investigating Atmospheric Drag Coefficient Composition Sensitivities - by Valerie Bernstein

Status of First Author: Student IN poster competition PhD

Authors: Valerie Bernstein, Marcin Pilinksi, Delores Knipp

Abstract: Atmospheric drag describes the perturbing force of the atmosphere on the orbital trajectories of Low Earth Orbit (LEO) objects and depends primarily on the spacecraft drag coefficient and the atmospheric mass density of the space environment. Both the drag coefficient and mass density are model dependent and thus contribute coupled model uncertainty to atmospheric drag estimates that can be challenging to distinguish. Atmospheric composition largely impacts the density and drag coefficients of LEO objects. In particular, recent work studying the effect of atmospheric helium on spacecraft drag coefficient estimates has shown that drag coefficients increase with a decreasing oxygen-to-helium ratio which can be highly variable at ~500 km altitudes around winter polar latitudes during solar minimum conditions. This response has been identified for drag coefficients computed for the Gravity Recovery and Climate Experiment (GRACE) satellite using a response surface empirical drag coefficient model based on the Cercignani-Lampis-Lord (CLL) gas-surface interaction framework trained by Test Particle Monte Carlo fitted to GRACE driven with atmospheric composition inputs from the Thermosphere-Ionosphere-Electrodynamics General Circulation Model (TIEGCM). We test whether these drag coefficient composition effects are commutable for other objects, since the response surface model is only fitted to the complex geometry of GRACE. To test the consistency of the CLL gas-surface interaction model, we select a set of compact, spherical tracking objects from the NORAD database at GRACE's altitude and derive atmospheric densities for these objects using their Two-Line Element (TLE) ephemeris information and CLL spherical drag coefficients. Taking the ratio of these CLL-dependent densities with atmospheric model densities from TIEGCM along the object's path and comparing with analogous density ratios for GRACE yields information about differences due to drag coefficient assumptions. This analysis will allow us to test the momentum and energy accommodation coefficient assumptions related to atmospheric composition of the CLL drag coefficient model and evaluate the validity of extending the effect of helium on GRACE drag coefficients to other orbiting objects independent of atmospheric density model dependencies.

IRRI02 - Characteristics of Es and Flayer observed by CODAR SeaSonde HF radar - by CHENG MING HONG

Status of First Author: Student IN poster competition Masters

Authors: Yen Hsyang Chu, Chien Ya Wang, Ching Lun Su

Abstract: CODAR SeaSonde radar is designed exclusively for ocean remote sensing. However, the HF radar wave reflected from Ionospheric Es and F layers at high elevation angle, which are transmitted by a monopole antenna equipped at a CODAR SeaSonde, may severely interfere the sea echoes in a range approximately from 100km to 400km. In order to realize the characteristics of the ionospheric interference on the Doppler spectra of the CODAR radar echoes over Taiwan area, we develop an algorithm to distinguish and separate the ionospheric interferences from the normal sea echoes in the Doppler spectral domain. The data employed in this study were taken from the CODAR radar located at DATAN (121.0329667N, 25.0327500) for 2016. We find that the patterns of the range-local time distributions of the

CODAR radar-detected Es layer echoes are in general agreement with those of the Es layer 3-meter field-aligned irregularity echoes observed by the Chung-Li VHF radar. In addition, the occurrences of the ionospheric interferences recorded by the CODAR radar are also highly correlated to the presences of the Es traces in ionograms observed by the ionosonde locate at Chung-Li City (121.247827E, 24.905056N). These features seem to suggest that the use of the ionosonde data combined with coherent VHF radar adjacent to the CODAR radar can provide useful information on the range and time of the ionospheric interferences occurred in the CODAR radar-detected sea echoes. By carefully removing the ionospheric interference, the data quality of the CODAR radar-estimated ocean current and wave parameters can be significantly improved.

IRRI03 - Global scintillation occurrence calculated by FORMOSAT-3/COSMIC S4-index - by Shih-Ping Chen

Status of First Author: Non-student PhD

Authors: Shih-Ping Chen, Jann-Yenq Liu, Wen-Hao Yeh, and Charles Lin

Abstract: A large amount of 1,441,527 F3/C RO S4 profiles sounded during 2007-2014 are used to update the F3CGS4 model calculating the probability of L-band S4 scintillation on the ground. This mega data is employed to calculate the median of converted ground-based S4 and the occurrence under various thresholds, and further find the conversion factor in various local times, seasons, and latitudes. The factor allows us to instantly calculate the S4 scintillation occurrence. Good agreements between our model simulations and previous observations indicate that the F3CGS4 can be used to calculate ground-based S4 **occurrence.**

IRRI04 - GNSS TEC and Scintillation Variations Following Solar Wind Dynamic Pressure Enhancement - by Thomas Coppeans

Status of First Author: Student IN poster competition Undergraduate

Authors: Shasha Zou, Jayachandran Thayyil, Anthea Coster, Allan Weatherwax

Abstract: Solar events such as CMEs and C!Rs can cause sharp increases in the dynamic pressure of the solar wind. When high pressure solar wind generated by these events impacts and compresses the Earth's magnetosphere transient plasma structures can be generated in the E and Flayers of the ionosphere globally. These plasma structures can diffract radio waves passing through them, an effect known as ionospheric scintillation, which can disrupt communication systems depending on them such as GNSS. Scintillation can subject GNSS to ranging errors, and in particularly bad cases, total loss of tracking. In this study we investigated the short-term (on the order of minutes) ionospheric response to solar wind dynamic pressure enhancements events, focusing on how these events manifest in GNSS disruption shortly after magnetospheric compression. We looked at events in a 4-year period from 2011 to 2014, and coordinated data from instruments provided by Antarctic scintillation receivers, the CHAIN network, AMPERE, SuperMAG, and global GPS TEC to understand the state of the ionosphere before and after these events. We carried out event studies on a case-by-case basis and on a statistical level for all events, and found higher levels of GNSS disruption starting within 5 minutes of magnetospheric compression, in some cases due to ionospheric scintillation. Additionally, we found that events where the solar wind had negative turning of the IMF Bz and large dynamic pressure increase were associated with higher GNSS disruption.

IRRI05 - The role of substorms in polar cap patch formation - by Lindsay Goodwin

Status of First Author: Non-student PhD

Authors: L. V. Goodwin, Y. Nishimura, B. J. Anderson, A. Coster, J. M. Ruohoniemi, and R. H. Varney

Abstract: A Tongue of Ionization (TOI) results when a large-scale change in the dayside convection pattern streams high-density dayside plasma into the polar cap. One process that changes convection is a southward turning of the Interplanetary Magnetic Field (IMF), but TOIs can also be observed during steady IMF conditions. Using dayside observations of total electron content, along with polar radar data from the Super Dual Auroral Radar Network (SuperDARN) and the Resolute Bay Incoherent Scatter Radar-North (RISR-N), this work investigates the potential role of substorms in the formation of TOIs and patches. In the absence of a southward turning of the IMF, this study finds that a substorm can trigger the creation of a TOI despite substorms being generally considered as a nightside phenomenon. When a substorm triggers a TOI, data from the Active Magnetosphere and Planetary Electrodynamics Response Experiment (AMPERE) show a sudden large-scale enhancement in the calculated dayside field-aligned currents and convection within 10 minutes of substorm onset. These results suggest the importance of substorms in patch/TOI formation when IMF triggers do not exist.

IRRI06 - Observations of Spatiotemporally local Structure in the Thermosphere over Alaska - by John Elliott

Status of First Author: Student IN poster competition student

Authors: John Elliott, Dr. Mark Conde - University of Alaska Fairbanks

Abstract: Using the Alaskan network of allsky viewing Fabry-Perot Interferometers, and geophysical inversion techniques, 3-component wind fields over the state of Alaska are inferred with high spatial resolution and a temporal resolution of a few minutes. Temporally local mesoscale structures are observed during both storm-time and quiet times, and are investigated as the result of being driven by geoeffective events.

IRRI07 - Auroral beads first stage of Substorm Onset - by Wendell Horton

Status of First Author: Non-student PhD

Authors: W. Horton, J. Derr, R. Wolf

Abstract: Auroral beads are the first stage of interchange-ballooning instability in nightside magnetotail that trigger substorm onsets. The nonlinear dynamics is calculated and compared with the observed beads given in Statistical characterisation of the growth and spatial scales of the substorm onset arc
N. M. E. Kalmoni, I. J. Rae et al. J. Geophys. Res. Space Physics, 120, doi:10.1002/2015JA021470.

IRRI08 - Equatorial Plasma Bubble Growth: Preliminary Numerical Assessment- by
Jonathon Smith

Status of First Author: Student IN poster competition PhD

Authors: Jonathon M. Smith

Abstract: The linear instability growth rate as derived by \cite{Sultan1996} provides a measure of the likelihood for bubble growth based on environmental factors along the geomagnetic flux tubes that plasma bubbles occupy. Previous numerical approaches for the estimation of the Rayleigh-Taylor linear growth rate utilizing observations of the vertical plasma drift and the SAMI2 model have explored the unique local time distribution of equatorial plasma bubble occurrence in specific seasons and longitudes during solar minimum \cite{Ajith2016, Zhan2017}. Here we discuss preliminary results of a broader exploration of this approach where the bubble growth rate as a function of local time is determined for and compared between zonal, seasonal, and annual periods.

IRRI09 - Analysis of plasma irregularities on a range of scintillation-scales using the Resolute Bay Incoherent Scatter Radars - by Leslie Lamarche

Status of First Author: Non-student PhD

Authors: Leslie J. Lamarche, Roger H. Varney, Carl L. Siefring

Abstract: Scintillation in the polar cap ionosphere is observed with a Coherent Electromagnetic Radio Tomography (CERTO) receiver while the Resolute Bay Incoherent Scatter Radars (RISR) provide background plasma conditions in a 3D volume. We interpret fluctuations in the VHF and UHF signal associated with mid-scale ionospheric structuring using 3D density gradients and plasma drift velocity vectors and calculate the maximum gradient drift instability growth rate. Plasma structuring is evident for any plasma density gradient, but sub-kilometer structures are less likely on the leading edge of polar patches, possibly due to a much faster diffusion rate for small scale structures. Structures are much more uniformly distributed around density enhancements that do not have clear leading and trailing edges. Although the gradient drift instability is an important factor in polar cap structuring, linear growth rates are most successful at predicting structuring around isolated density enhancements in consistent plasma flows. For more general density gradients, the time history of a plasma parcel and local diffusion rates must also be considered.

IRRI10 - A study of Polar Cap Patches using RISR - by Robert Irvin

Status of First Author: Student IN poster competition PhD

Authors: R.J. Irvin, Y.T. Nishimura, L.V. Goodwin

Abstract: Polar Cap Patches are structured (100-1000km) Electron density enhancement in the Polar Cap that are at least twice the background. The various formation mechanisms of patches and their relative dominance has been a subject of debate. Here, we consider two formation mechanisms that have received significant attention, local particle precipitation and poleward propagation of photoionized plasma. We apply a patch detection algorithm (developed in Perry et al. 2018) to RISR data to characterize the formation mechanisms of Polar Cap Patches.

IRRI11 - The Farley-Buneman Spectrum in 2-D and 3-D PIC Simulations - by Matthew Young

Status of First Author: Non-student PhD

Authors: Matthew Young, Meers Oppenheim, Yakov Dimant

Abstract: Since the 1960s, the Farley-Buneman instability, also known as the modified two-stream instability, has been a topic of scrutiny within the ionospheric community. The intervening years have seen significant progress in the linear theory of this instability, its relation to other instabilities, and its observational signatures. However, the saturation mechanism and nonlinear behavior remain open topics. This paper presents 2-D and 3-D fully kinetic simulations of the Farley-Buneman instability in the high latitude ionosphere, at three different simulated altitudes: 107, 110, and 113 km. Simulated irregularity amplitude exhibits growth and saturation stages in all runs, but the growth stage differs between 2-D and 3-D runs. The saturated stage of 2-D runs exhibits a power-law with slope -3.4 to -4.2 at meter scales and a shallower but nonzero slope at longer wavelengths. The saturated stage of 3-D runs exhibits a power-law with slope -5.1 to -5.9 at meter scales and a nearly flat spectrum at longer wavelengths. Images in the perpendicular plane show that the flow angle is always larger than 90° . Thermal instabilities appear to contribute to the nonzero flow angle at lower altitudes but the flow angle approaches the direction of electron-ion relative drift as altitude increases. This work predicts that the saturated amplitude of Farley-Buneman irregularities should exhibit a flat spectrum with a knee at the wavelength of peak growth and a flow angle at least as large as the deviation of relative drift from $\mathbf{E}_0 \times \mathbf{B}_0$.

IRRI12 - Multi-scale Observations of High-Latitude Ionosphere Plasma Transport During Oct. 12, 2016 Geomagnetic Storm - by Jiaen Ren

Status of First Author: Student IN poster competition PhD

Authors: Jiaen Ren, Shasha Zou

Abstract: Solar-produced concentrated F-region plasma can be transported from the mid-latitude region into the polar cap during geomagnetically disturbed period, generating strong plasma irregularities like polar cap patches and causing scintillation and outages of space communications and degraded performance for Global Navigation Satellite System (GNSS) at polar latitudes. Mitigation techniques are limited because we are still not clear about what governs the generation, structure and propagation of those high-density plasma. Multi-scale observations of the plasma structure and transport will provide key information in the study of the highly-debated patches production mechanisms process and their scintillation effects. This study investigates the dynamic transport process of ionosphere concentrated plasma from the mid-latitude subauroral region into the high-latitude polar cap in the Northern Hemisphere during the Oct. 12, 2016 Geomagnetic Storm. In this work, the OPS TEC data and the SuperDARN convection map are used to study large-scale plasma transport. During the storm main phase, an extended period of strong southward IMF Bz condition caused the expansion of the high-latitude ionosphere convection pattern, transporting the storm-enhanced density (SED) into the polar cap. Tongue of ionization and several polar cap patches are observed by the OPS TEC map, the Resolute Bay incoherent scatter radar (RISR) and the DMSP satellites, and their temporal evolution and multi-scale structures are investigated. The scintillation effects associated with the plasma irregularities are also studied using data from the Canadian High Arctic Ionospheric Network (CHAIN). Moreover, a patch segmentation process shown in the OPS TEC map is suggested to be caused by a sudden eastward flow enhancement ~ 2 km/s at the dayside cusp inflow region observed by the Sondrestrom incoherent scatter radar, which is suggested to be associated with a sudden and short period of IMF By negative excursion.

IRRI13 - A Global View of Ionospheric Response Impacts on Kinematic GPS Positioning during the 2015 St Patrick's Day Storm - by Zhe Yang

Status of First Author: Non-student PhD

Authors: Zhe Yang, Jade Morton

Abstract: This study for the first time presents a global view of ionospheric disturbances impacts on kinematic GPS Precise Point Positioning (PPP) solutions during the March 17, 2015 St. Patrick's Day geomagnetic storm. More than 5200 GNSS stations from worldwide networks are utilized. The results show that the spatial-temporal variation of the kinematic PPP errors is strongly correlated with that of the ionospheric plasma irregularities observed during the storm. On the day of the commencement of the storm, i.e., 17 March 2015, a meter level of accuracy can be observed over both Northern and Southern Hemisphere, but a long-lasting period (up to several hours) of the large errors (up to 10 meters) is predominantly seen over high latitudes of North America and European regions. The results would be valuable for predict impact on GNSS-based kinematic applications when severe ionospheric storm prevails.

IRRI14 - A case study to understand the ionospheric structures over Poker Flat Research Range using forward propagation model SIGMA and Configuration Space Model - by Pralay Raj Vaggu

Status of First Author: Student IN poster competition PhD

Authors: K.B Deshpande, S. Datta-Barau, C.L. Rina, A. Lopez

Abstract: The electron density structures cause fluctuations in the signal phase and amplitude, so called scintillation which affects the Global Navigation Satellite System (GNSS) signals. Characterization of the irregularities can help us to mitigate the scintillation effects on any satellite-based system. It is well known that the phase scintillations are predominantly observed in high latitude regions. Data obtained from GNSS receivers during geomagnetically active period along with the three-dimensional (3-D) global scintillation model "Satellite-beacon Ionospheric-scintillation Global Model of the upper Atmosphere" (SIGMA) is used to characterize the small - medium scale high latitude ionospheric irregularities which are likely to produce GNSS signal scintillations (K.B. Deshpande et.al., 2014). SIGMA simulates the signal that propagates through the irregularities from moving satellite to the ground receiver. An inverse method is used to derive the irregularity parameters by comparing the high rate GNSS observations to the modelled outputs (K.B. Deshpande et.al., 2016). SIGMA runs over a uniform four dimensional grid to fit the simulated power spectral density (PSD) to the observed PSD. We optimize the SIGMA PSD to agree with the observed PSD using four free inputs such as electron number density (N_e), spectral Index, drift velocity magnitude and direction. The auxiliary data from Scintillation Auroral OPS Array (SAGA) sited at Poker Flat Research Range, Alaska (S. Datta-Barua et.al., 2015) provides a good estimate of the drift velocity. We also rely upon SuperDARN and Incoherent Scatter Radar (ISR) for velocity and electron density estimates. Our aim is to improve the input parameters of the model using optimal estimators. In this study, we analyse the ionospheric structures over Poker Flat during November 16th 2014 over a 30 s interval after 10:30 UT that shows a good signatures of phase and amplitude scintillations. Inverse method used in estimating the electron number density of 1012 electrons/m³ well matches with ISR estimates. The well-known spaced receiver technique using SAGA cluster provides SIGMA with an optimal value for drift velocity. Of 750 m/s in northwest direction. Furthermore, the spectral density functions (SDFs), the average intensity of Fourier transformations of the electron density structures from Configuration Space Model (Charles Rina et. al., 2018), which generates structure realizations from random collections of striations are used to interpret the peak electron density which can be a good estimate of an irregularity distribution incorporated into SIGMA. Enforcing the irregularity parameters obtained using above techniques gives us a

better estimation of signal propagation that reflects into the characteristic features of electron density structures in the ionosphere. Such a study can help us to understand and estimate the ionospheric structures that affect all the satellite-based systems.

IRRI15 - MELISSA studies of equatorial spread F: Post-midnight events - by Weijia Zhan

Status of First Author: Student IN poster competition PhD

Authors: Weijia Zhan, Fabiano Rodrigues

Abstract: Most of the ionospheric radar observations in South America come from the Jicamarca Radio Observatory, in the western sector. The deployment of the 50 MHz RESCO radar and subsequently the 30 MHz FCI radar in Sao Luis, Brazil allowed observations in the eastern sector. Only FCI, however, was capable of measuring F-region echoes. Despite operating for several years (2000-2012), the FCI radar made observations only during daytime and pre-midnight hours with a few exceptions. Here, we describe a 30 MHz radar system that replaced the FCI radar, and present results of full-night F-region observations. This radar system is referred to as Measurements of Equatorial and Low-latitude Ionospheric irregularities over Sao Luis, South America (MELISSA) and made observations between March 2014 and 2018. We focus, on this presentation, on the detection of post-midnight F-region echoes. We also examine the spectral features of such echoes and compared these features with those associated with typical pre-midnight equatorial spread F (ESF) events.

IRRI16 - FDTD Modeling of HF Waves Through Ionospheric Plasma Irregularities - by Dallin Smith

Status of First Author: Student NOT in poster competition Masters

Authors: Cheryl Huang, Jamesina Simpson, Eugene Dao

Abstract: Radio scintillation and scattering at high latitudes of the earth can occur when polar cap patches are present. These patches, usually formed during periods of southward interplanetary magnetic field (IMF), enter by the dayside cusp and convect in the antisunward direction having densities 2-10 times the background densities. Irregularities are caused by gradient drift instabilities (GDI) and are observed throughout the patch. While the patch can range from 100 to 1000 km in size, the irregularities can range from meters to 10's of km. Various difficulties may arise in attempting to model scintillation and scattering of electromagnetic waves by these irregularities due to (1) modeling the complicated geometric structures of the irregularities, (2) simulating electromagnetic waves in a magnetized plasma environment, (3) and accounting for computational efficiency and accuracy. The finite difference time domain (FDTD) method is a new approach to simulate propagation of electromagnetic waves throughout the patch. Irregularities and patch profiles were generated based on Defense Meteorological Satellite Program (DMSP) data. The sizes of the irregularities can be defined by a Weibull distribution function which is used to create a probability density function for irregularities in a given patch size. The patch profiles were added to a FDTD model having a dipole source in the high frequency region. Features such as spread F were captured in the simulation as small sized irregularities scattered the waves. Experimental spread F observations were used to validate the FDTD model. A ray tracing model was compared to the FDTD model with the same irregularity and patch profile to give contrast between the two modeling methods.

IRRI7 - Overview of scintillation events due to E region and F region as inferred from SAGA - by Aurora Lopez

Status of First Author: Student IN poster competition Masters

Authors: A. Lopez!, S. Datta-Barna!, K. B. Deshpande, V. PralayRaj, D. L. Hampton, and G. S. Bust

Abstract: Scintillations in Global Navigation Satellite System (GNSS) received signals at the ground are caused by the variation in electron density in the ionosphere when they travel through it. Satellite communication or ground systems can be affected by this solar activity and charged particle flow in the ionosphere. However, these rapid fluctuations in power and/or phase in the received signal does have the advantage of allowing the study of the properties and the physical mechanisms that produce the irregularities. An array of closely-distributed GNSS receivers is used to monitor the scintillation. SAGA (Scintillation Auroral Global Positioning System (GPS) Array) is located in the auroral zone at Poker Flat Research Range, Alaska. In previous work, there have been analysis of a couple of events where completed case studies were made. The drift velocity [Su et al., 2017a], the height and thickness of the scattering layer were estimated [Su et al., 2017b]. On the other hand, a survey of scintillation events was conducted from 2014-2015, in which these cases were determined and classified according to frequency of the GPS (L1 or L2), region E or F of the scattering layer and amplitude or/and phase fluctuation of the signal [Sreenivash et al., in revision]. However, a broad analysis of events has not been conducted. In this work, we study different scintillation events, at GPS L1 or L2, amplitude-only, phase-only or phase and amplitude fluctuation and occurred in the E region or F region, with the data of SAGA. The objective is to determine an approximation of the velocity drift magnitude and orientation and the height and thickness of the scattering layer of all these multiple events. This last estimation will provide the layer in which the scintillation occurred, the E or the F layer, which will help to refine the classification of the scintillation events. These estimates are compared with collocated JSR measurements. V. Sreenivash, Y. Su, and S. Datta-Barna. "Detection, Classification, and Attribution of Auroral GPS Scintillation to Ionospheric Scattering Layer", in revision. Y. Su, S. Datta-Barna, G. S. Bust, and K. B. Deshpande (2017a), "Distributed sensing of ionospheric irregularities with a GNSS receiver array," Radio Science, 52, 8, August 2017, pp. 988-1003, doi:10.1002/2017RS006331. Y. Su, G. S. Bust, K. B. Deshpande, and S. Datta-Barna, (2017b), "Estimating height and thickness of an ionospheric irregularity layer with a closely-spaced GNSS receiver array", Proceedings of the 30th International Technical Meeting of The Satellite Division of the Institute of Navigation (ION GNSS+ 2017), Portland, Oregon, September 2017, pp. 3375-3388.

IRRI18 - Multi-scale density irregularities at mid-latitudes: GPS scintillation imaging - by Sebastijan Mrak

Status of First Author: Student IN poster competition Masters

Authors: Sebastijan Mrak, Joshua Semeter, Marc Hairston, Douglas Drab

Abstract: Global Positioning Systems (GPS) receivers from contiguous US are used to derive maps of Total Electron Content (TEC), differential TEC (dTEC) and amplitude/phase scintillation. The high-rate (1-Hz) UNAVCO database is used to derive the GPS scintillation. It is shown, that small-scale (~100 km -- a few km) irregularities are embedded within meso-scale (~100 km) TEC structures, during geomagnetically disturbed times. The results reveal that the small- to meso- scale irregularities are entirely M1-coupling driven phenomenon, confined to the mid- latitude ionosphere.

IRRI19- Hybrid Simulations of Farley Buneman Instabilities in the Auroral E Region - by Enrique Rojas Villalba

Status of First Author: Student IN poster competition Masters

Authors: Enrique Rojas Villalba, David Hysell

Abstract: The magnetosphere couples with the high latitude ionosphere through the earth's magnetic field lines. This coupling occurs mainly through energetic particle precipitations and electromagnetic fields. In the auroral E region, these processes cause Hall currents that drive Farley Buneman instabilities, generating a spectrum of field-aligned plasma density irregularities (FAI). Even though coherent radar backscatter from auroral E region PAIs can be measured with great accuracy and precision, the theoretical framework to relate the echo characteristics to ionospheric state variables and convection electric fields is still limited. Furthermore, comparisons between the convection patterns derived from Doppler spectral moments and from JSR measurements are difficult because of the lower spatial and temporal resolution of the latter. Meanwhile, rocket data are finely resolved in space and time but scarce. The limited data available to validate a convection model motivates the need for new validation criteria. We present preliminary results from hybrid simulations of Farley Buneman waves based on a continuous approach. Electrons were treated using fluid theory, and ions using the unmagnetized Vlasov equation with a BGK collision term. Preliminary results demonstrate reasonable qualitative and quantitative agreement with comparable PIC code simulations. We investigate phase speed saturation and examine whether the phase speeds of the waves scale with the background electric field in the way observed by the coherent scatter radar. We also try to quantify wave turning effects, examine whether wave heating is commensurate with incoherent scatter radar observations and determine the dominant wavelength of the waves.

IRRI20 - An effective technique for isolation of Traveling Ionospheric Disturbances from GNSS-derived Total Electron Content measurements - by Anahita Shahbazi

Status of First Author: Student IN poster competition Masters

Authors: Jihye Park, Hoda Tahami

Abstract: The theoretical and experimental studies have shown that natural hazards trigger abnormal variations in electron concentration of the ionosphere, referred to as Traveling Ionospheric Disturbance (TID). Recalling the dispersive nature of the ionosphere to the VHF radio signals, Global Navigation Satellite System (GNSS) can be advantageous to investigate TIDs by extracting Total Electron Contents (TEC) from dual-frequency observations. To isolate the TIDs from TEC measurements, advanced signal processing technique is required. One of the most critical steps in the advanced signal processing technique is detrending process due to the low amplitude of TID waveforms and uncertainties of the GNSS observations. However, the TEC detrending procedure is extremely challenging considering the high levels of dynamic activities in the ionosphere. Specially, frequent oscillations and abrupt disturbances following a natural hazard make the detrending procedure more complicated. Thus, we developed a new detrending method by combining natural neighbor interpolation and leave-one-out technique. In the proposed detrending approach, the leave-one-out technique performs a statistical analysis to enhance the confidence of trend estimation by natural neighbor interpolation while distinctively highlights the TIDs in the detrended TECs. For this analysis, we examined the ionospheric responses to Kusatsu-Shiranesan volcanic eruption in Japan on 23 January 2018. The investigation of the detrended TEC signals revealed that the dominant TEC trends were estimated with a standard deviation of 0.075 and an average of -0.001 TECU. As an additional signal processing skill, wavelet-based denoising technique was also applied to the detrended TECs. This denoising step enhanced the TID isolation process so that weak TIDs, which may be hidden by the observational noise, were successfully depicted. We characterized the eruption-induced TIDs with an average propagation velocity of 529.894 m/s during a time period of 7.5-32.5 minutes after the eruption and considered them as the immediate response of the ionosphere to the explosion. Finally,

coherence analysis of the detected TIDs verified the performance of detrending methodology in TID isolation by a coefficient of 78.8% for the Japanese volcanic eruption.

IRRU1 - ROTI estimation by dual-frequency GPS receiver measurements during magnetic storms- by Jack Wang

Status of First Author: Student IN poster competition PhD

Authors: Yunxiang Liu, Zhe Yang, Ian Collett, Yu (Jade) Morton, Scott Palo

Abstract: GNSS remote sensing can be used to characterize the overall structure of the ionosphere and perturbations of that structure. In this research, we will use a novel algorithm to accurately estimate the TEC using dual-frequency GPS receiver measurements. The objective is to qualitatively understand the high-latitude ionospheric response to the geomagnetic storm. We find that the rate of TEC index (ROTI) has significant variations when the horizontal magnetic field has strong fluctuations. Our result demonstrates that the ROTI can be a valuable indicator for the perturbation of the navigation system caused by the ionospheric irregularity.

IRRU2 - Peak Height Distributions of Equatorial Ionospheric Irregularities deduced from the C/NOFS satellite mission - by Dev Joshi

Status of First Author: Student IN poster competition

Authors: Dev Joshi, John Retterer, Patrick Roddy, Chaosong Huang, Keith Groves

Abstract: The low-latitude ionosphere is characterized by large-scale instabilities in the post-sunset hours due to the distinct geometry of the earth's magnetic field lines at the equator. The magnetic field lines are horizontal at the equator contributing to the high vertical drift velocity of the plasma bubbles growing from the bottomside of the ionospheric F-region. The phenomenon, commonly known as equatorial spread F, is an important problem in aeronomy as it can cause radio wave scintillation effects representing the most critical impacts of space weather on man-made technologies, such as satellite communications and global navigation satellite systems (GNSS). Here, we present results from naturally occurring instabilities in the equatorial ionosphere. The data from the Communications/Navigations Outage Forecasting System (C/NOFS) satellite mission -- the Air Force Research Laboratory (AFRL) / the National Aeronautics and Space Administration (NASA) -- has been analyzed to investigate the characteristics of equatorial ionospheric irregularities from in situ observations. We present a comprehensive investigation on the variation of peak apex-altitude distribution of equatorial ionospheric irregularities with solar activity supported by modeling, simulation and comparisons with ground- and space-based in situ density observations. We also analyze Physics Based Model (PBMOD) ionospheric model results to determine if a physics-based model can reproduce the observed dependence of bubble height on solar activity.

ITIT01 - Observations of Second Harmonic Generation in Stimulated Electromagnetic Emissions during Ionospheric Heating - by Augustine Yellu

Status of First Author: Student NOT in poster competition PhD

Authors: Augustine Yellu, Wayne Scales, Paul Bernhardt, Carl Siefring, Alireza Mahmoudian

Abstract: Secondary radiation produced when a powerful high-frequency HF electromagnetic wave from a ground-based transmit station interacts with the ionosphere, known as stimulated electromagnetic emissions (SEEs), provides important ionospheric diagnostics such as electron temperature, ion mass, density and turbulence spatial/temporal characteristics. Important distinctions can be made in the physical processes producing narrowband stimulated electromagnetic emissions (NSEEs), which exist within ± 1 kHz of the pump wave frequency, and wideband stimulated electromagnetic emissions (WSEEs) which exist outside ± 1 kHz of the pump wave frequency. Second harmonic generation (SHG) refers to the occurrence of SEEs in the vicinity of twice the pump wave frequency. SHG has been developed into a powerful diagnostic tool in Laser Plasma Interactions (LPI) yielding diagnostics such as the velocity of plasma resonance region, scale length of electron density inhomogeneity, etc. and can potentially produce similar diagnostics for ionospheric heating experiments. Only very recently has this potential been explored in detail. Observations of SHG during ionospheric heating experiments at the High Frequency Active Auroral Research Program facility (HAARP), Gakona AK in September 2017 were reported in 2018. The reported results were from an experiment in which the transmit frequency was stepped near the 3rd harmonic of the electron gyrofrequency. At each frequency, the transmit power was linearly ramped from 3.6% to 80% of the maximum capacity of 3.6 MW. Highlights of the reported observations were the occurrence of SEE within 30 Hz of the second harmonic of the pump wave frequency which showed a similar transmit power dependence as NSEEs due to stimulated Brillouin scatter (SBS) within 30 Hz of the pump wave frequency and the suppression of SEEs for pumping very near the 3rd harmonic of the electron gyrofrequency. In this poster, the reported observations will be compared with results from another experiment conducted during the same September 2017 HAARP campaign. The experiment is similar to the experiment described above except that the transmit power was maintained at 2.88 MW corresponding to 80% of the maximum capacity during the entire heating cycle at each frequency. A key observation from this experiment is that NSEEs near the pump wave frequency due to SBS and the downshifted decay line near the second harmonic are present during only the first few seconds of the heating cycle. Electromagnetic Particle-in-Cell PIC plasma simulations are utilized to interpret this behavior in terms of density cavity development due to nonlinear development of ion acoustic waves associated with the SBS. Also reported in this poster are observations from experiments conducted at HAARP in March 2019 during which the transmit frequency was stepped near the 2nd harmonic of the electron gyrofrequency, the transmit power either maintained at a constant 2.88 MW or linearly ramped from 101.5 kW to 2.88 MW and the transmit beam direction either maintained constant or stepped. In many respects, the observations for 2nd gyro-heating show consistency with the September 2017 3rd gyro-heating and underscore the potential of SHG as a powerful ionospheric diagnostic tool.

ITIT02 - Performance Assessment and Improvements for the FORMOSAT-5 Onboard Orbit Propagator Using GPS Ephemeris - by CHI-TING LIAO

Status of First Author: Student IN poster competition PhD (checked)

Authors: Chi-Ting Liao, Loren C. Chang, Wen-Lung Chiang, Ming-Yu Yeh

Abstract: Launched in 2017, FORMOSAT-5 is a spacecraft located on a 720 km Sun synchronous orbit carrying indigenously developed payloads for Earth observation and in-situ ionospheric measurements. The FORMOSAT-5 attitude and orbit control subsystem (AOCS) contains a navigation filter utilizing a numerical orbit propagator to provide estimates of spacecraft inertial position and velocity when the onboard GPS receiver is not available. Times during which the onboard GPS is available provide a unique

opportunity to assess the performance of the orbit propagator, as well as to explore further improvements. In this paper, we report the variation of the FORMOSAT-5 orbit propagation error during different seasons, as well as geomagnetic and solar activity conditions. The effects on orbit propagation error by introducing drag effects from various empirical thermospheric models is also explored. The results will be used to improve navigation and tracking functions for future Taiwanese satellites, including those of the six FORMOSAT-7/COSMIC-2 satellites, which will be located at lower orbits subject to increased perturbation from drag. The results also provide insight into the neutral density modeling capability of current empirical thermosphere models, which are also a key tool for understanding thermosphere and ionosphere variability.

ITIT03 - Ionospheric Echoes Detection in Digital Ionograms Using Convolutional Neural Networks - by Cesar De La Jara

Status of First Author: Student NOT in poster competition Masters

Authors: Cesar De La Jara, Cesar Olivares

Abstract: An ionogram is a graph that shows the distance that a vertically transmitted wave, of a given frequency, travels before returning to the earth. The ionogram is shaped by making a trace of this distance, which is called virtual height, against the frequency of the transmitted wave. Along with the echoes of the ionosphere, ionograms usually contain a large amount of noise of different nature, that must be removed in order to extract useful information. In the present work, we propose to use a convolutional neural network model to improve the quality of the information obtained from digital ionograms, compared to that using image processing and machine learning techniques, in the generation of electronic density profiles. A data set of more than 900,000 ionograms from 5 ionospheric observation stations is available to use.

ITIT04 - False Detection of Ionosphere-Induced GNSS Cycle Slips at High-Latitude - by Brian Breitsch

Status of First Author: Student IN poster competition PhD

Authors: Brian Breitsch, Jade Morton

Abstract: Ionosphere scintillation is notorious for causing some of the most severe disturbances in measurements by Global Navigation Satellite System (GNSS) receivers. This phenomenon occurs when radio signals that propagate through ionosphere plasma irregularities exhibit strong phase and amplitude fluctuations. The scintillation that high-latitude ground receivers experience is characterized by strong phase fluctuations as measured by the sigma-phi scintillation index, but weak fluctuations in signal amplitude as measured by the S4 scintillation index. This is in contrast to scintillation observations made at low-latitude that are associated with diffractive signal fluctuations that contain deep fades in signal amplitude and associated fast phase changes. These diffractive fluctuations (that only really occur for ground receivers at low-latitudes) can induce diffraction-induced phase transitions--jumps in the measured signal phase that look like traditional GNSS cycle slips but are real propagation effects from the disturbed ionosphere. In contrast, such diffractive fluctuations do not occur at high-latitude, and by looking at sigma-phi variations in correspondence to structure in dual-frequency total electron content (TEC) fluctuations, it is apparent that much of "scintillation" observed at high-latitude may be more correctly characterized as fast moving ionosphere plasma structures. In studying such structures that induce strong phase dynamics, the introduction of cycle slip artifacts by the GNSS receiver can become a serious problem. Knowing that diffractive fluctuations do not occur at high-latitude, can we correctly detect receiver-induced cycle slips while also avoiding false alarms due to strong TEC dynamics? There is a significant body of work on

dealing with GNSS cycle slips. Many of these approaches make use of multi-frequency geometry-free phase combinations to detect outliers in epoch-to-epoch phase differences. These outliers are then used to estimate the integer ambiguities, often using the least-squares ambiguity decorrelation adjustment technique (LAMBDA). As noted in (Banville 2010, 2013), (Jiao 2013), the phase trend due to ionosphere total electron content (TEC) often cannot be ignored, and a TEC rate variable must also be estimated. A common pitfall of these algorithms is that they fail to detect or properly estimate certain cycle slip combinations, especially during strong phase noise or large variations in ionosphere TEC. (Li 2019) addresses this issue by making use of a window of observations when estimating the change in cycle ambiguities. This approach is promising when it comes to difficult-to-estimate cycle slip combinations; e.g. (1, 1, 1) for GPS L1, L2, and L5 signals. However, validation of their approach does not address false alarms during particularly strong high-latitude ionosphere disturbances. In this work, we look at periods of strong phase variations (as measured by the sigma-phi index) for high-latitude GNSS receivers in order to assess how well these cycle slip detection algorithms can avoid false classification of cycle slips due to strong TEC variations. We plan to specifically address the algorithm outlined in (Li 2019). Evaluation of the performance during strong ionosphere irregularities at high-latitudes will help to assess whether such algorithms adequately capture ionosphere dynamics in order to properly identify cycle slip occurrence. We will also explore if there is room for tighter constraints on TEC and ionosphere structure dynamics, which are approximated by polynomial models in current cycle slip detection methods. Ultimately, it may be necessary to develop adaptive algorithms for better ionosphere-related cycle slip detection/estimation, which will necessitate strong understanding of the scale and speed of high-latitude ionosphere irregularities. Moreover, if current cycle slip detection methods have too-high false alarm rates, it will strengthen the demand for ionosphere irregularity drift forecasting.

!TITOS - Electron collision effects on ISR temperature measurements of the ionosphere. - by William Longley

Status of First Author: Student NOT in poster competition Masters

Authors: William J. Longley, Philip J. Erickson, Meers M. Oppenheim, Juha Vierinen, Yakov S. Dimant

Abstract: Incoherent scatter radars (ISR) estimate the electron and ion temperatures in the ionosphere by fitting measured spectra of ion-acoustic waves to forward models. For radars looking at aspect angles within 5° of perpendicular to the Earth's magnetic field, the magnetic field constrains electron movement and Coulomb collisions add an additional source of damping that narrows the spectra. Fitting the collisionally narrowed spectra to collisionless forward models leads to errors or underestimates of the plasma temperatures. This work presents the first fully kinetic particle-in-cell simulations of ISR spectra with collisional damping by velocity dependent electron-electron and electron-ion collisions. For aspect angles between 0.5° and 2° off perpendicular, the damping effects of electron-ion and electron-electron collisions are the same and the resulting spectra are narrower than what current theories predict. For aspect angles larger than 3° away from perpendicular, the simulations with electron-ion collisions match collisionless ISR theory well, but spectra with electron-electron collisions are narrower than theory predicts at aspect angles as large as 5° away from perpendicular. At all aspect angles the particle-in-cell simulations produce narrower spectra than previous simulations using single particle displacement statistics. Current forward models used for fitting measured spectra at Jicamarca and Millstone Hill do not account for the additional damping by electron-electron collisions, leading to underestimates of electron temperatures by as much as 25% at these radars. The particle-in-cell simulations are compared to spectra measured at small aspect angles by the fully steerable MISA antenna at Millstone Hill. The data from Millstone Hill show that current fitting routines fail to converge on accurate temperature measurements at aspect angles of 3.6° or smaller, in agreement with the results from particle-in-cell simulations.

ITIT06 - Northern Alaska Receiver Comparison - by Meghan LeMay

Status of First Author: Student IN poster competition PhD

Authors: Meghan LeMay, Josh Semeter

Abstract: Will present side-by-side analysis comparing the NetRS and low-power Septentrio results for the northern Alaska seismic array stations including variance of navigation solution during geomagnetic activity.

ITIT07 - Three Dimensional Mapping of Lightning Produced Ionospheric Reflections - by Joseph Malins

Status of First Author: Student NOT in poster competition Masters

Authors: Joseph Malins, Kenneth Obenberger, Greg B. Taylor, Jayce Dowell

Abstract: The powerful HF/VHF radio emissions that occur during lightning flashes can be used as a signal of opportunity to study the bottom side ionosphere. The lightning emission is bright, broad spectrum, and short in duration, providing an ideal signal of opportunity for making ionograms. This study continues previous work in \citeA{Oben_Lightning}, where the direct line of sight signal from lightning can be cross correlated with MHz frequency radio telescope observations to reveal ionogram traces created from the reflected lightning signals. This process was further developed to automate the process and create new techniques to detect the lightning signal. By using the Long Wavelength Array Sevilleta radio telescope as an interferometer, the point of reflection of the lightning signal on the ionosphere can be pinpointed, instantaneously revealing density gradients within the ionosphere on minute time scales. We also explore the minimum size stations required for the application of this technique.

ITIT08 - Terahertz emission by the nonlinear coupling of Laser and Kinetic Alfvén wave in a magnetized plasma - by Himani Dewan

Status of First Author: Student IN poster competition Masters

Authors: Himani Dewan, M.Singh, R.Uma, R.P Sharma.

Abstract: In this paper we report analytical modelling for parametric decay instability of high intensity elliptically-polarized laser beam (ω). The perpendicular laser beam parametrically decays into Whistler wave and Kinetic Alfvén Wave (KAW). The beating mechanism, of oscillatory electrons pertaining to KAW in parallel direction is induced due to the nonlinear coupling of elliptically-polarized laser velocity and whistler wave density perturbation. As a result terahertz radiations are eventually created due to this three-wave interaction process. The necessary phase matching condition is obtained by constructing the phase diagram (parallelogram) which simultaneously satisfies the conservation of momentum-energy. The coefficients for the coupling of this parametric decay process and the growth rate of this instability is deduced. We extensively study different cases to inquire the effect of variations in characteristics of laser beam on THz output.

ITIT09 - Gridded Retarding Ion Drift Sensor (GRIDS) for PetitSat - by Benjamin Obom

Status of First Author: Student NOT in poster competition Masters

Authors: Benjamin Obom, Ryan Davidson

Abstract: PetitSat is a cube satellite (CubeSat) mission engineered to collect in situ measurements of plasma density enhancements in the low/mid-latitude of the ionosphere. The overarching goal of the mission is to uncover what driving mechanisms are responsible for the formation of these enhancements. To do this, the satellite will carry two instruments to take plasma and neutral measurements. One of these instruments is a unique combination of a retarding potential analyzer (RPA) and an ion drift meter (IDM). Together they are dubbed the Gridded Retarding Ion Drift Sensor (GRIDS). GRIDS will collect data pertaining to the density, velocity, ion species ratios, and temperature of the plasma through which it passes. Coupled with the data from the other instrument aboard petitSat, insights into the physics driving this phenomenon in the ionosphere will improve.

ITIT10 - Using two dimensional autocorrelation method to improve the performance of automatic algorithm on ionogram - by KAI-Jun KE

Status of First Author: Student IN poster competition Masters

Authors: Kai-Jun Ke, Kang-Hung Wu, Yen-Hsyang Chu, Ching-Lun Su

Abstract: A new ionosonde is under construction at Chung-Li VHF radar station on the campus of National Central University in Taiwan. We develop our own data processing algorithm to automatically retrieve ionospheric parameters of different sublayers from observed ionogram traces in nearly real time. In addition to the conventional image analysis technique and empirical orthogonal function (EOF), we use two-dimensional autocorrelation function to identify and separate the ordinary (O-) wave from extraordinary (X-) wave traces for further analysis. A comparison between ionospheric parameters retrieved from the automatic processing algorithm developed in this study and those obtained from manually scaling ionograms shows that the use of two-dimensional autocorrelation function combined with image analysis and EOF methods can achieve reliable and accurate ionospheric parameters.

ITIT11 - Daedalus: ESA's Earth Explorer 10 mission candidate for thermosphere-ionosphere studies - by Alex Hoffmann

Status of First Author: Non-student PhD

Authors: Alex Hoffmann, Arnaud Lecuyot, Theodoros Sarris, The Daedalus Teams

Abstract: Daedalus is a thermosphere-ionosphere explorer mission concept, selected by the European Space Agency for Phase-0 feasibility studies, competing with two other candidates for implementation as the tenth ESA Earth Explorer flagship mission. Daedalus (doi.org/10.5194/ge-2019-3) aims at quantifying key electrodynamics and Sun-Earth coupling processes that determine structure, composition and dynamics of the transition region between the upper atmosphere and space. Daedalus targets the under-sampled region between <120 and 200 km of altitude with a suite of in situ instruments to measure plasma density

and temperature, ion drift, neutral density, temperature and winds, ion and neutral composition, as well as the electric and magnetic fields and precipitating particles, all during both quiet and active geomagnetic conditions. This shall contribute to quantifying the amount of energy deposited into the upper atmosphere, in terms of Joule heating and energetic particle precipitation, and more generally, to furthering our understanding of Sun-Earth coupling. The original mission concept relied on an elliptical orbit in conjunction with the periodic release of expendable "sub-satellites"; periodically ejected and miniaturized spacecraft with a suite of instruments to complement those of the primary spacecraft in the lowest altitudes of this vertical range, in addition to providing multi-point observations of key geophysical parameters. During the feasibility studies, various design and implementation options will be considered, and the scope and requirements of the mission will be gradually refined. This poster focuses on a high-level early mission concept overview and background, the programmatic framework of the feasibility study, community involvement and opportunities, and on the underlying science and system definition studies launched in spring 2019. The aim is to foster the exchange of ideas, to explore synergies, and to gather early community thoughts, needs and contributions in support of the mission definition.

ITIT12 - Ion acoustic terahertz generation by a femtosecond laser pulse in plasma - by

Narender Kumar

Status of First Author: Student IN poster competition Masters

Authors: Narender Kumar, R. Uma, R. P. Sharma.

Abstract: A p-polarised laser impinged on an inhomogeneous plasma (at an angle to density gradient) mode converts to a plasma wave near the critical layer. The plasma wave survives much after the laser pulse is gone. The plasma wave heats the electrons near the critical layer. The sudden rise in plasma electron temperature causes a rise in plasma pressure and emission of ion acoustic wave at the frequency lower than the ion plasma frequency. It appears to be a mechanism for ion acoustic wave (in Terahertz range) observed in an experiment.

ITIT13 - In-situ electron density from Langmuir waves: the influence of the spacecraft wake - by Hassan Akbari

Status of First Author: Non-student PhD

Authors: Hassanali Akbari, Laila Andersson, David J. Andrews, David Malaspina, Mehdi Benna, Robert Ergun

Abstract: Results from active sounding in the Martian ionosphere---produced by the Langmuir probe and Waves instrument aboard the MAVEN spacecraft---are presented. The electric field spectral measurements obtained shortly after subjecting the plasma to a 3.3 V white noise signal (transmission power <100 uW) shows, under some circumstances, a resonance line at frequencies slightly below the electron plasma frequency of the local ionosphere. The observed resonance line is interpreted to originate from the plasma waves excited within the wake behind the spacecraft. The results, not previously reported in earlier missions, uncover an important phenomenon in in-situ electron density derivation from Langmuir waves. These results, furthermore, provide the possibility of investigating the characteristics of the electron wake in a novel manner. By analyzing the frequency of the observed resonance line, with respect to the electron

and ion densities derived from the Langmuir probe's I-V sweeps and the onboard ion instrument, we infer that the ratio of the electron density inside the spacecraft wake to that of the ambient ionosphere decreases from ~ 1 to 0.4 as the spacecraft descends in altitude from 450 km to 185 km. In this interval the electron density, electron temperature, and Debye length vary from 1×10^3 to $1.5 \times 10^4 \text{ cm}^{-3}$, 2500 to 1200 K, and 0.1 to 0.02 m, respectively. The spacecraft velocity remains in the vicinity of 4 km/s.

ITIT14 - Comparison of Ionospheric Electron Density Retrieved from Spire Global Radio Occultation Data with Arecibo Incoherent Scatter Radar and Ionosonde Measurements - by Victoriya Forsythe

Status of First Author: Non-student PhD

Authors: Victoriya Forsythe and Don Hampton

Abstract: Radio occultation (RO) has been proven to be a powerful technique for ionospheric electron density profile (EDP) retrieval. Commercial GNSS-RO ionospheric measurements collected by Spire's 3U CubeSat constellation could significantly improve the determination of the global ionospheric state. In this work, the EDPs retrieved from Spire total electron content (TEC) measurements using Abel inversion corrected by horizontal asymmetry are compared to Arecibo electron density measurements. Good agreement is observed in case-by-case EDP comparison. The information about F2 layer peak and height obtained from Spire RO data is also compared to ionosonde measurements at 70 stations around the globe from DIAS network.

ITIT15 - Space Weather Atmospheric Reconfigurable Multiscale Experiment Cubesat - by Scott Palo

Status of First Author: Non-student PhD

Authors: Scott Palo, Marcin Pilinski, Jeffrey Thayer, Simone D'Amico, Saeed Latif, Kristina Lemmer, Whitney Lohmeyer, Glenn Lightsey

Abstract: In spring 2019 the National Science Foundation expanded their cubesat program program to include the Directorate for Engineering, the Directorate for Computer & Information Science & Engineering in addition to the Directorate for Geosciences. A new approach, the NSF Ideas Lab, was utilized where a group of 28 interdisciplinary researchers met for a week to share ideas and develop forward looking cubesat mission concepts. The outcome of the meeting was four mission concepts of which SWARM-EX is one. The bold vision for SWARM-EX is to develop a reconfigurable cubesat swarm which can be utilized to address a range wide range of ionospheric/thermospheric spatial/temporal coupling questions as outlined in recent decadal reports. Groups of cubesats ranging from 3 to 12 or more cubesats operate in close proximity (hundreds of meters to hundreds of km) making similar measurements. The groups or formations are in similar orbital planes and at similar attitude and can be reconfigured on orbit to make science measurements on the desired temporal and spatial scale. Dozens of such formations would be operating simultaneously in a range of orbital planes and altitudes creating a distributed array of small satellite instruments (DASS!). This constellation or swarm would be used to address compelling ionospheric/thermospheric research. The SWARM-EX cubesat is a capable 2.5U bus with space to accommodate a 0.5U space weather instrument. The core bus includes a high performance attitude determination, propulsion, a UHF radio for command, control and crosslinks, a high rate CDMA X-band radio for downlink, GPS and a core avionics suite. An initial phase flying 3 cubesats with identical space weather instruments is proposed to demonstrate the capability of the SWARM-EX approach.

ITIT16 - On Deriving Self-consistent, High-accuracy Mass Density Measurements - by Piyush Mehta

Status of First Author: Non-student PhD

Authors: Valerie Bernstien, Delores Knipp

Abstract: High-accuracy thermospheric mass density estimates derived from measurements of orbital drag on-board the CHAMP and GRACE satellites have been the workhorse of upper atmospheric research for close to two decades. These estimates use drag coefficients (CD) computed with neutral species composition from some empirical model that provides global estimates by combining diffusive equilibrium profiles with lower boundary number density estimates that can contain errors. The derived density estimates are then used to generate corrections to the model(s) used to derive them, making the process circular in nature. Recent work on self-consistent calibration of empirical models provide insight into the errors in lower boundary estimates and temperature profiles. This work investigates its impact on the process of deriving density estimates from measurements of acceleration onboard satellites by recomputing density estimates using composition and temperature from the assimilated state. Results indicate that the current process of estimating density may be inconsistent as the recomputed density estimates can have significant differences from the original density estimates, especially during solar minimum conditions, because of significant redistribution of lighter species like helium and inaccurate models.

ITIT17 - The Chinese Meridian Project for Space Weather Monitoring - by ZhiQing Chen

Status of First Author: Non-student PhD

Authors: ZhiQing Chen

Abstract: The Chinese Meridian Space Weather Monitoring Project (Meridian Project) is a ground-based geospace monitoring facility in China, consisting of 15 observation stations located roughly along 120°E longitude and 30°N latitude. It was designed to monitor key parameters from the ground to upper atmosphere and ionosphere. Being equipped with various types of instruments, the project is the most comprehensive among peers in the world. Since formal operation from 2012, great research progress has been made on major topics facing the space weather community. In 2018, the Chinese government approved an even more ambitious program, to make a grand upgrade to the current project. That is the phase II of the project. It will deploy more stations to better cover China's territory, and build a stereo monitoring capability covering all space spheres of the solar terrestrial system. Addition to the existent two monitoring chains, another two chains will be established along 100°E longitude and 40°N latitude respectively, forming a Two-cross network configuration. The construction of phase II project is estimated to start in 2019 and finish in 2022. On completion of the construction, the Chinese Meridian Project will run nearly 300 instruments that deployed at 31 stations. Instruments include ordinary ones, such as magnetometers, FPs, Digsondes. Also many innovative and powerful instrument will be developed, such as radioheliographs with a very wide combined frequency band, a 3-station phased incoherent radar to make 3-D measurement of the ionosphere, and a synthetic aperture helium lidar to measure atmosphere density up to 1000km.

\\IDIT01 - A Machine Learning-based study of TEC variations in response to large equinoctial geomagnetic storms - by Shantanab Debchoudhury

Status of First Author: Non-student PhD

Authors: Shantanab Debchoudhury, Disha Sardana, Gregory D. Earle

Abstract: The evolution of the total electron content (TEC) in the ionosphere in the aftermath of a large geomagnetic storm is complex and depends on a number of factors. In this study, we focus on the TEC response in the US sector. We choose a dataset of large solar storms in the equinox periods of solar cycles 23 & 24 (2000-2015). The key variable studied is the difference between the post-storm TEC value and an average from 5 quiet days during the same month. This is correlated with various storm parameters, including the onset time of the storm, the duration of the storm, its intensity, and the rate of change of the ring current response. The contiguous US area is further divided into regions of positive and negative magnetic declinations. We use machine learning techniques to quantify the relative importance of the measured storm characteristics on the temporal behavior of the average TEC variation in each region throughout the storm period. This data-driven machine learning approach reveals correlations between the storm signatures and the resulting TEC variations.

\\IDIT02 - A Study of Solar Flare Effects on Mid and High Latitude Radio Wave Propagation using SuperDARN - by Shibaji Chakraborty

Status of First Author: Student NOT in poster competition Masters

Authors: S. Chakraborty, J.M. Ruohoniemi, and J.B. H. Baker

Abstract: A prolonged study is underway to improve the understanding of the D-region response to solar flare and its effects on HF propagation. OTH communication is strongly dependent on the state of the ionosphere, which is fragile to solar X-ray flares. Signal properties of Super Dual Auroral Radar Network (SuperDARN) are altered (strongly attenuated and changes apparent phase) during solar flares, commonly known as Short-Wave Fadeout or SWF. During an SWF the number of SuperDARN ground-scatter echoes drops suddenly ("I min) and sharply followed by an apparent increase in Doppler velocity (also known as "Doppler Flash"), often to near zero, reflecting disruption. HF propagation data (SuperDARN backscatter) obtained during SWF events are analyzed here to validate and improve the performance of HF absorption models, such as, currently operational Space Weather Prediction Center (SWPC) D-region Absorption model (DRAP) and CCMC physical AbbyNormal model. The SWPC DRAP model is an empirical model providing real-time global predictions of D-region absorption, and the physical Absorption by the D and lower E Region of HF Signals with Normal Incidence (AbbyNormal) model is based on simple D-region physics and provides near real-time predictions of mid-latitude D-region HF absorption. Also, the study tries to propose a relatively newer model to estimate the frequency anomaly that can be seen in the SuperDARN data before the signal loss. In this study we used data from a sub-network of SuperDARN radars across North America to validate the consistency of the absorption models, also to model the frequency anomalies and find the ionospheric sources of Doppler flash phenomenon. This study will help us to estimate different physical parameters of ionosphere such as electron density, collision frequency, absorption coefficients, the response time of D-region, etc. and validate the model based on the SuperDARN observations.

MDIT03 - A High-Resolution Model of Exospheric Temperatures - by Daniel Weimer

Status of First Author: Non-student PhD

Authors: Daniel R. Weimer

Abstract: A high-resolution model of exospheric temperatures has been developed, with the objective of predicting the global mapping of exospheric temperatures with unprecedented accuracy. These temperatures can be used to predict neutral densities. This new model is based on measurements of the neutral densities on the CHAMP, GRACE, and Swarm satellites, which were sorted into grid cells on a triangulated, spherical mesh, based on geographic latitude and local solar time (longitude). Each grid cell uses a separate set of coefficients, obtained by a least-error fit of the data within that cell. Several versions of model functions have been tried, with one of the better results obtained using parameters for the day-of-year, Universal Time, solar indices M10.7 and Y10.7, and the total power of nitric oxide emissions, as measured with the SABER instrument on the TIMED satellite. Accuracy is improved with the addition of input parameters for the total Poynting flux flowing into the Northern and Southern hemispheres, obtained from IMF measurements using an empirical model. Slightly better results were obtained with a version that uses the total Poynting flux in a derivation of the global change in the exospheric temperature as a function of time, that is incorporated into the calculation within each grid cell. The maps of the exospheric temperature that are produced show significant variability in the polar regions, that are strongly modulated by the time-of-day, due to the rotation of the magnetic poles around the geographic pole.

MDIT04 - Solving for the Thermal Conductivity Coefficients Experimentally - by Brandon Ponder

Status of First Author: Student IN poster competition PhD

Authors: Aaron Ridley

Abstract: We compare the Global Ionosphere Thermosphere Model (GITM) mass density output to the data available from the Challenging Minisatellite Payload (CHAMP) mission in order to parameterize the unmeasurable constants of Earth's atmosphere. The thermal conduction of the upper atmosphere cannot be measured with an instrument and therefore poses challenges to determine the value we should consider when solving the energy equation. Since GITM takes thermal conduction of O species and O₂ species as inputs, we can, with a couple runs, predict the output of GITM without using the computing time. This allows us to match the background state during CHAMP's orbits and improve future GITM runs by defining a solution set τ_0 the thermal conduction parameters.

MDIT05 - Retrieval of Thermospheric Atomic Nitrogen using Preassociative Nitric Oxide Delta Band Emissions - by Justin Yonker

Status of First Author: Non-student PhD

Authors: Charlotte Cassell, Scott M. Bailey

Abstract: Ground state atomic nitrogen N(4S) is an abundant thermospheric species with an important role in the global energy budget. It exhibits the largest diurnal density variability of any thermospheric species, ranging nearly six orders of magnitude from midnight to noon. As the dominant loss process for E-region nitric oxide (NO), the cannibalistic reaction between N(4S) and NO $\text{NO} + \text{N}(4\text{S}) \rightarrow \text{N}_2 + \text{O}(3\text{P})$

is crucial in controlling the rate of NO cooling at 5.3 microns in response to geomagnetic forcing. Yet quantification of the above process remains a frontier as N(4S) is among the most poorly measured thermospheric species [McCoy, 1983]. As a result of this paucity of observational data, empirical models such as the Naval Research Laboratory Mass Spectrometer and Incoherent Scatter Empirical 2000 model (NRLMSISE-00, Picone et al, [2002]), are in sharp disagreement with physics-based, photochemical models of the atomic nitrogen density. This project takes a first step in remedying this deficiency by using measurements of the Remote Atmospheric and Ionospheric Detection System (RAIDS) to retrieve the N(4S) density. RAIDS was a spectrometer suite built at the Naval Research Laboratory that flew aboard the International Space Station from 2009-2011 [Budzien et al, 2010]. Its observations of the preassociative NO delta band emission near 190 nm are here used with NRLMSISE 0(3P) to retrieve the N(4S) density.

MDIT06 - Parametric estimation of neutral hydrogen density using proton continuity balance with TIMED/GUVI and SAMI3 - by Pratik Joshi

Status of First Author: Student IN poster competition PhD

Authors: Pratik P. Joshi, Lara Waldrop

Abstract: Imbalances in the nearly resonant charge exchange between H⁺, O, O⁺ and H⁺ are dominant drivers of H⁺ and O⁺ transport between the plasmasphere and topside ionosphere. In this work, we present a new technique to derive neutral atomic hydrogen density, [H], which is poorly known yet and is critically important to MLT chemistry and atmospheric escape. The new technique is based on parametric solution of the proton continuity equation including charge-exchange-driven transport that accounts for violation in charge-exchange equilibrium. Our data constraints on the proton continuity equation include atomic oxygen density [O] derived from the inversion of 135.6 nm OI emission measured by TIMED/GUVI and coincident H⁺ and O⁺ densities and velocities, and ion temperature specification from the SAMI3 ionospheric model. The variability of the derived [H] is presented as a function of local time, space and solar activity for the middle and lower latitudes (-60 deg to 60 deg). The derived [H] profiles are compared with NRLMSISE-00 and their agreement with TIMED/GUVI observations of its resonantly scattered Lyman- α emission at 121.6 nm will be evaluated. The proposed technique exhibits promising performance as an independent method for [H] estimation and consequent assessment of potential thermospheric model bias.

MDIT07 - Source Investigation and analysis of TIDs over equatorial and low-latitude regions - by Olusegun Jonah

Status of First Author: Non-student PhD

Authors: A. Coster, S. Zhang, L. Goncharenko, P. J. Erickson, B. Rideout, E. R. de Paula.

Abstract: Traveling ionospheric disturbances (TIDs) are wave-like disturbances in ionospheric plasma density. They are often observed during both quiet (Medium scale TID) and geomagnetic disturbed (Large Scale TID) conditions. Their amplitudes can be up to 10% of the background plasma density and their presence provides a challenge to existing radio wave propagation theories. In this study, we investigate how TIDs generation mechanism and propagation vary with different plasma background densities during various geophysical conditions. The transequatorial coupling of TIDs north and south hemispheres are also investigated with respect to attenuation and propagation characteristics. We show that TID properties during transequatorial events may be substantially affected by background neutral wind perturbation (owing to disturbance dynamo effects), vertical and horizontal velocity which are seasonal dependent. Our

study observations occurred during both quiet and geomagnetic disturbed periods using multiple ground and space borne instruments, such as: Magnetometers, GNSS receivers as well as the DMSP and SWARM satellite missions in low Earth orbit.

MDITOS-Dynamic response of ionospheric plasma density to the geomagnetic storm of 22-23 June 2015 - by Olusegun Jonah

Status of First Author: Non-student PhD

Authors: John Bosco Habarulema, Elvira Astafyeva, Endawoke Yizengaw, Olusegun F. Jonah, Geoff Crowley, Andy Gisler, and Victoria Coffey

Abstract: On June 21--22, 2015, three consecutive interplanetary shocks slammed into the Earth's magnetosphere. A multi-instrument approach comprising of observations, data analysis, and modeling is used in the present study to examine the global ionospheric response. Results show that enhanced storm-time processes produced major total electron content (TEC) variations at different latitudes, longitudes, and phases of the storm. Multiple equatorward and poleward propagating traveling ionospheric disturbances (TIDs) were detected from the TEC data. The equatorward propagating TIDs are consistent with vertical neutral winds simulated from TIE-GCM, however, the model was not able to produce poleward TIDs. We find that a combination of driving processes include enhanced high-latitude injection, prompt penetration electric fields, disturbance dynamo effect, neutral winds, and composition changes were acting at different stages of the storm.

MDIT09 - Ionosphere responses to the May 2017 magnetic storm: Results from multi-instrumental observations over the Chinese sector - by Lei Liu

Status of First Author: Student IN poster competition PhD

Authors: Lei Liu; Shasha Zou; Ercha A; Yibin Yao

Abstract: An intense geomagnetic storm occurred at 1530UT on 27 May 2017, which was caused by a corona mass ejection (CME) generated on 23 May. In this study, we investigate ionosphere responses to this storm over the Chinese sector by using multi-instrumental observations, including ground-based GNSS network, COSMIC RO electron density profiles (EDP), and in-situ plasma density observations provided by Swarm and DMSP missions. (1) Two positive ionospheric storm periods are observed: The first one was observed at mid-low latitudes on May 28, and the most intense positive ionospheric storm occurred around 0200-0700UT (dayside). Also, the second and smaller-scale of positive storm occurred during 1000-1600UT on May 29. These two positive storms were clearly induced by southward turning of interplanetary magnetic field (IMF) Bz. (2) A negative storm occurred during 0200-1800UT on May 30, which could be attributed to the thermospheric composition change as shown by the decrease of O/N2 ratio from TIMED/GUY. (3) Small-scale nighttime plasma bubbles/depletions by using filtered TEC and ROTI map were observed at longitude sector -110° E below -35°N at 1600-1800UT on May 28. We suggested that the storm time PPEF with long-lasting southward IMF Bz during this time periods may help to create favorable condition for these bubbles. (4) We observed ionosphere disturbances/perturbations by using filtered GNSS TEC during this storm, but no clear zonal propagation of traveling ionospheric disturbances (TID) were detected over the Chinese sector for this storm.

MDITI O - Comparative testing of electron density assimilative models- by Leonard Thomas

Status of First Author: Non-student

Authors: T.A. Leonard, Poppy L. Martin, Natasha K. Jackson-Booth

Abstract: This poster presents comparisons of ionospheric assimilative models with empirical background models, evaluating their ability to provide accurate profiles of electron density. These models assimilate various data sources using either the Gauss-Markov Kalman filter approach or Bayesian inference to deviate from the background model. Comparative testing methods comprise modified Taylor diagrams to compare second-order statistics of f_oF_2 values, and vertical difference profiles to compare month-long averages of electron content values by altitude against vertical ionosonde data. A description of the testing scenario used is also given.

MITCOI - CAPER-2 and TRICE-2 Sounding Rocket Investigations: Wave-Particle and Wave-Wave Interactions in the Polar Cusp - by Chrystal Moser

Status of First Author: Student IN poster competition Undergraduate (check pending)

Authors: James LaBelle, Craig Kletzing, Scott Bounds, John Bonnell, Stephen Fuselier, Joran Moen

Abstract: The CAPER-2 and TRICE-2 sounding rockets launched 4 January 2019 and 8 December 2018, respectively, into the cusp of earth's magnetic field as part of the Grand Challenge Initiative: Cusp. The Cusp Alfvén Precipitating Electron Rocket (CAPER-2) launched into active cusp aurora, achieving an apogee of 774 km. Its goal is to study wave-particle interactions in the upper ionosphere to understand the process by which energy is transferred between cusp electrons and both Alfvén waves and Langmuir waves. The Twin Rockets to Investigate Cusp Electrodynamics (TRICE-2) launched two minutes apart into active cusp aurora, achieving apogees of 1042 km and 756 km. The principle goal of the two rockets is to observe reconnection signatures that originate on the dayside magnetosphere. Both of these missions carried high frequency instruments to examine auroral radio emissions ranging from 100kHz-5MHz allowing for fine structures within the spectra to be observed. Preliminary results show events at frequencies corresponding to whistler, Langmuir, and upper hybrid waves. For example, there are distinct striped features in the whistler frequency range that have been observed on previous rockets but have yet to be explained. There are structured waves just below the time-varying upper hybrid frequency with spacing of roughly 5 kHz. There are numerous intense and highly structured waves at the plasma frequency. On CAPER-2 a wave-particle correlator analyzes energy flow between these waves and electrons in eight energy ranges. These experiments will provide advances in understanding wave-particle and wave-wave interactions in the polar cusp.

MITC02 - Poynting Flux from DMSP in Auroral Boundary Coordinates - by Liam Kilcommons

Status of First Author: Non-student Undergraduate

Authors: Liam Kilcommons, Delores Knipp

Abstract: We use magnetic perturbations and ion drift velocity from the Defense Meteorology Satellite Program (DMSP) FJ5, F16, F17 and F18 spacecraft to compute the downward directed DC Poynting Flux ($S = 1/\mu_0 \text{Ex} \cdot \text{dB}$) at 850 km for several years under varying solar cycle conditions. To reduce the bias from instrument artifacts in the Poynting flux, we use baseline-corrected "Level-2" magnetometer data (Kilcommons et al. 2017) and filter the Ion Drift Meter (IDM) and Retarding Potential Analyzer (RPA)

measurements using the University of Texas, Dallas (UTD) quality flags. Additionally, we apply a baseline correction to the ion drift measurements to reduce bias. To investigate partitioning of energy deposition between the auroral region and the polar cap, we use the DMSP electron precipitation auroral boundary detection algorithm (Kilcommons et al., 2017) to divide each DMSP orbit into polar cap, auroral and subauroral regions, and bin the corresponding Poynting flux both in standard magnetic coordinates and also relative to these boundaries. We show statistical maps of ion convection velocity, average Poynting Flux strength, likelihood of strong flux, and other electrodynamic parameters both in magnetic and auroral boundary coordinates. We particularly highlight the strong influence of the sign of IMF By on the location of Poynting flux electromagnetic energy deposition.

MITC03 - Kinetic modeling of auroral ion outflows - by Robert Albarran

Status of First Author: Student IN poster competition PhD

Authors: Robert Albarran, Matthew Zettergren

Abstract: The VISIONS (Visualizing Ion Outflow via Neutral atom imaging during a Substorm) sounding rocket was launched on Feb. 7, 2013 at 8:21 UTC from Poker Flat, Alaska, into an auroral substorm with the objective of identifying the drivers and dynamics of the ion outflow below 1000km. Energetic ion data from the VISIONS polar cap boundary crossing show evidence of an ion "pressure cooker" effect whereby ions energized via transverse heating in the topside ionosphere travel upward and are impeded by a parallel potential structure at higher altitudes. VISIONS was also instrumented with an energetic neutral atom (ENA) detector which measured neutral particles (-50-100 eV energy) presumably produced by charge-exchange with the energized outflowing ions. Hence, inferences about ion outflow may be made via remotely-sensing measurements of ENAs. This investigation focuses on modeling energetic outflowing ion distributions observed by VISIONS using a kinetic model. This kinetic model traces large numbers of individual particles, using a guiding-center approximation, in order to allow calculation of ion distribution functions and moments. For the present study we include mirror and parallel electric field forces, and a source of ion cyclotron resonance (ICR) wave heating, thought to be central to the transverse energization of ions. The model is initiated with a steady-state ion density altitude profile and Maxwellian velocity distribution characterizing the initial phase-space conditions for multiple particle trajectories. This project serves to advance our understanding of the drivers and particle dynamics in the auroral ionosphere and to improve data analysis methods for future sounding rocket and satellite missions.

MITC04 - A Hydrodynamic Model for Plasmasphere Refilling Following Geomagnetic Storms - by Kausik Chatterjee

Status of First Author: Non-student PhD

Authors: Kausik Chatterjee, Robert W. Schunk

Abstract: The refilling of the plasmasphere following a geomagnetic storm remains one of the longstanding problems involving ionosphere-magnetosphere coupling. Both diffusion and hydrodynamic approximations have been adopted for the modeling and solution of this problem. The diffusion approximation neglects the nonlinear inertial term in the momentum equation and so this approximation is not rigorously valid immediately after a storm. The principle focus of this work is the formulation and development of a hydrodynamic refilling model (that includes the nonlinear inertial term) using the flux-corrected transport method, a numerical method that is extremely well-suited to handling nonlinear

problems with shocks and discontinuities. In a previous study, this model has been validated against exact analytical benchmark problems and in this study, the model is used to describe plasmasphere refilling. The plasma transport equations are solved along one-dimensional closed magnetic field lines that connect conjugate ionospheres and the model currently includes three ions (H^+ , O^+ , He^+) and two neutral (O , H) species. In this study, each ion species under consideration has been modeled as two separate streams emanating from the conjugate hemispheres and the model correctly predicts supersonic ion speeds and the presence of high levels of helium during the early hours of refilling. The ultimate objective of this research is the development of a three-dimensional model for the plasmasphere refilling problem, and with additional development, the same methodology can be applied to the study of other complex space plasma coupling problems in closed flux tube geometries.

MITC05 - Time History Observations of Barium Releases from the C-REX Mission and their Relevance to the Ionosphere CUSP Region Density Anomaly - by Matthew Blandin

Status of First Author: Student IN poster competition PhD

Authors: Matthew Blandin, Don Hampton, Mark Conde, Peter Delamere

Abstract: In the thermosphere of the Earth's geomagnetic cusp a neutral density up-welling ranging from a 30% to a 100% increase has been observed, while no production mechanism has been confirmed that can explain such a significant and stable anomaly. This phenomenon has enough interest to the space physics community that there is a joint NASA/ESA sounding rocket campaign underway to examine this cusp region in more detail. In November of 2014 the C-REX mission, one of the first dedicated projects to studying this phenomenon, released 10 barium/strontium tracer clouds into the cusp thermosphere between 190 and 425 km altitude. These tracer clouds were recorded from Ny-Alesund, Svalbard using a Nikon D810 DSLR camera, providing a time history of the releases. The goal is to quantify the observed effects on the stopping power, expansion rates, and diffusion rates of the clouds and compare them to the expected results determined using the MSIS-E-90 atmospheric model. Due to the neutral density up-welling, significant deviations in these parameters are expected, which will be used to further quantify the scale of the neutral density anomaly.

MITC06 - Characteristics of meso-scale structures in the high-latitude ionosphere - by Yun-Ju Chen

Status of First Author: Non-student PhD

Authors: Yun-Ju Chen, Roderick Heelis

Abstract: An investigation of meso-scale (100-600 km) flow perturbations and accompanying electron precipitation and field-aligned current in the high-latitude ionosphere is presented. These localized features are expected to give us new insights into magnetosphere-ionosphere coupling process. In this study, ion drift, particle precipitation and magnetic field measurements from the Defense Meteorological Satellite Program (DMSP) F1 6, F1 7 and F18 satellite are utilized to identify these meso-scale features. The flow perturbation and the closure flow can be basically described by single cell or two-cell configuration of the electrostatic potential. Local minima in the potential distribution are associated with electron precipitation and upward field-aligned current. However, the potential, precipitation and field-aligned current are dependent on the sense of circulation in the meso-scale feature. The characteristics of meso-scale structures in terms of the potential, conductance and field-aligned current provide a more complete picture of these

coupled properties, the extra energy inputs into the ionosphere and the effective area over which they are delivered.

MITC07 - Small-scale convection cells in the polar ionosphere: Origins and implications for energy dissipation - by Joaquin Diaz Pena

Status of First Author: Student IN poster competition PhD

Authors: Joaquin Diaz Pena, Joshua L Semeter, Toshi Nishimura, Marc Hairstone

Abstract: Magnetic re-connection can be considered the main driver of fast ionospheric flows channels that become part of the convection cells, which in turn can generate F region patches that move across the polar cap. By using satellite data from the Defense Meteorological Satellite Program (DMSP), such events can be studied using energy flux, velocity, density and temperature measurements to obtain an approximate boundary for the polar cap, flow movement at the ionosphere, and temperature enhancements or depletions. DMSP is ideal for spatial measurements over the polar caps given its low earth, and the always dawn to dusk orbit. The inclusion of measurements from Incoherent Scatter Radars (!SR) such as Poker Flat (PFISR) and Resolute Bay (RISR), which can acquire spatial and temporal information together with coverage, resolution, and uncertainty defined by the experimental mode, add an extra layer of understanding by looking at conjugated points with DMSP passes over or close to the beams of the electronically steerable radars. These two types of measurement have very different space-time sampling rates, resolutions, and uncertainties Ionospheric flow channels and F region patches coming down due to high latitude re-connection caused by the slightly northward IMF of January 24th, 2012, are measured using both DMSP and RISR. Perpendicular flows from RISR can be obtained using several oblique beams to estimate the flow and data products. Conjunction points are presented to analyze the complementary relationship between the respective data sets to obtain new insights into the complex flow patterns excited by high-latitude magnetic re-connection events, including: large enhancements in density, dynamics off region patches, changes on the ExB drift due to re-connection, and temperature variations with a preliminary Joule heating analysis using available data.

MITCOS - An examination of inner-magnetosphere shielding by Region-2 Field-Aligned Currents - by Bharat Kunduri

Status of First Author: Non-student PhD

Authors: B. Kunduri, J.B. H. Baker, J.M. Ruohoniemi

Abstract: It has long been speculated that the inner-magnetosphere is shielded from the cross-tail electric field by a dusk-dawn directed shielding electric field, generated by charge separation associated with inner magnetosphere Alfvén layers and the region-2 Field Aligned Currents (FACs). However, during periods of large and rapid fluctuations of the Interplanetary Magnetic Field, the shielding balance is likely perturbed, resulting in either under-shielding or over-shielding of the inner-magnetosphere. In this study, we present a methodology to use the relative imbalance between Region-I and Region-2 FACs, derived from AMPERE measurements, as a proxy for inner magnetosphere shielding. Specifically, we identify periods of rapid changes in the interplanetary electric field and utilize large-scale measurements of FACs from the AMPERE project in conjunction with electric fields in the mid-latitude ionosphere from SuperDARN to examine the extent to which the inner magnetosphere is under-lover- shielded and determine the relevant time scales under different geomagnetic conditions.

MITC09 - Alfvénic heating as a source of thermospheric density anomalies - by Benjamin Hogan

Status of First Author: Student IN poster competition PhD

Authors: Benjamin Hogan, William Lotko

Abstract: Thermospheric density anomalies were recorded by the CHAMP satellite in the high-latitude noon and midnight regions at altitudes near 400 km (1). The anomalies can exceed the predictions of empirical density models such as MSIS by as much as 100%. Alfvénic electromagnetic power flows, broadband electron precipitation, and ionospheric ion outflows are present in regions similar to those of the air density anomalies and may be causally related. A preliminary analysis (2) of Alfvén wave energy deposition in a model cusp ionosphere suggests that F-region Alfvénic energy deposition may be sufficient to produce the anomalies measured by CHAMP, especially when accompanied by low-energy electron precipitation. **In** contrast with quasistatic Joule heating, which depends primarily on the imposed electric field and Pedersen conductivity, Alfvénic Joule heating is also controlled by the ion mass density profile, most importantly at altitudes near its F-region peak value. We have extended the Lotko-Zhang analysis (2) to determine diurnal, seasonal and solar cycle variations in Alfvén wave heating of the ionosphere-thermosphere for ambient conductivities and wave speeds derived from the IR1 and MSIS empirical models. We consider broadband Alfvén wave driving with simulated satellite Doppler frequencies ranging from 0.05 to 15 Hz and with amplitudes and spectral content consistent with low-altitude satellite measurements. We have also surveyed the ionosphere environment derived from empirical models at cusp latitudes to correlate conditions that will lead to intense F-region Alfvénic heating.

MITC10 - Electric Drift Morphology According to Van Allen Probes Measurements - by Solene Lejosne

Status of First Author: Non-student PhD

Authors: Forrest Mozer

Abstract: The instruments onboard the Van Allen Probes are the first to be accurate enough to deliver reliable, near-equatorial measurements of the electric drift in the plasmasphere, even below three Earth radii. The objective of this presentation is to discuss how we could leverage the new visibility offered by this unique database of electric drift measurements to advance our understanding of the **MIT coupling**.

MITCH - Determine the role of nitrogen ions in the ionospheric outflow - by Meiyun Lin

Status of First Author: Student IN poster competition PhD

Authors: Raluca Ilie, Alex Glozer

Abstract: Knowledge of ion composition in the terrestrial ionosphere and magnetosphere is crucial to understand the plasma dynamics in the Earth's magnetosphere-ionosphere system. The discovery of O^+ and N^+ in the ionosphere and magnetosphere hinted to the connection between the ionospheric and magnetospheric plasma, suggesting that the ionosphere acts as a reservoir for the magnetospheric plasma. However, most instruments flying in space couldn't distinguish between O^+ and N^+ due to their close masses, and therefore the contribution of N^+ to the magnetosphere-ionosphere system has remained unknown. Idealized simulation results with the Hot Electron Ion Drift Integrator (HEIDI) point out the importance of N^+ in the ring current. The presence of N^+ , even small amount of it, changes the magnetospheric dynamics and alters the ENA fluxes. In order to track the behavior and determine the role of N^+ in magnetosphere-ionosphere system, we properly include N^+ ions into the Polar Wind Outflow Model (PWOM). Preliminary simulation results indicate that the presence of N^+ in the ionospheric outflow can change ionospheric dynamics in the low altitudes where chemical reaction and collision are dominated. Our initial simulation results suggest that N^+ and O^+ are required to describe separately in the magnetosphere-ionosphere system, since they obey different chemical and physical reactions.

MITC12 - On the spectra and emission altitudes of STEVE: A case study - by Jun Liang

Status of First Author: Non-student PhD

Authors: E. Donovan, M. Connors, D. Gillies, B. Gallardo-Lacourt, E. Spanswick, J. Brian, and D. Hampton

Abstract: We report a event study of STEVE on July 17, 2018, with focus on the spectra and emission altitudes of STEVE. We find that the STEVE in the event comprises of two traces, one at higher elevation angle and the other at lower elevation angle. The two traces closely follow each in their southward motion, and eventually merge to one near the zenith. Spectrograph measurements show that both STEVE traces are characterized by enhancements over a broad range of wavelength, i.e., airglow continuum, consistent with the initial findings in Gillies et al. [2019]. The two STEVE traces however, differ on their red-line (630nm) component: The higher-elevation STEVE contains substantial red-line enhancement over background, while the lower-elevation STEVE does not. Based upon triangulation using multiple optical instruments, including AUGSO and REGO imagers, FESO and spectrometer, we evaluate that the two STEVE traces are likely emitted from distinctly different altitudes: the higher-elevation STEVE comes from ~250 km altitude, while the lower-elevation comes from 110-150 km altitude. This finding may impose profound implications on the possible underlying mechanisms of STEVE.

MITC13 - Hemispheric Asymmetries in High-latitude Field-aligned Currents (FACs) Revealed by Inverse and Assimilative Analysis of AMPERE Magnetometer Data - by Yining Shi

Status of First Author: Student IN poster competition PhD

Authors: Yining Shi, Delores Knipp, Tomoko Matsuo, Brian Anderson

Abstract: High-latitude field-aligned current (FAC) and magnetic potential patterns are reconstructed with optimal interpolation (OI) method using magnetic perturbation data provided by the NSF-funded Active Magnetosphere and Planetary Electrodynamics Response Experiment (AMPERE) program. Background model and background error covariance used in the OI method is estimated from -100 days of AMPERE data for difference solar wind drivers. Four event studies during both solstice and equinox are presented here to illustrate some hemispheric asymmetries seen in the FAC and magnetic potential patterns. Well-known asymmetries such as IMF B_y effect and seasonal differences due to dipole tilt are revealed in our patterns. In addition, we find that the IMF B_x can also cause hemispheric asymmetry in FACs and magnetic potential when B_x is comparable or larger than B_y and B_z under weak solar wind drivers or northward B_z conditions. Total currents calculated from the patterns indicate that under weak solar wind driver conditions, the northern hemisphere shows more intense FACs and magnetic potential on average where the total currents in the northern hemisphere can be 20% to 30% higher than in the southern hemisphere. This asymmetry may be caused by the difference in Earth's magnetic field strength and the larger offset between the geographic pole and geomagnetic pole in the southern hemisphere.

MITC14 - On the factors that control plasmaspheric ion composition - by Naomi Maruyama

Status of First Author: Non-student PhD

Authors: Naomi Maruyama, Mei-Ching Fok, Phil Richards, Dmytro Kotov, Yuki Obana, Yoshizumi Miyoshi, George Khazanov

Abstract: The profiles of cold heavy ions in the plasmasphere have distinctly different characteristics from those of light ions. There are suggested mechanisms but they do not yet fully explain the observed profiles. The purpose of this study is to examine the various underlying physical processes that control cold ion composition in the plasmasphere. We investigate the physical processes that could explain the cold heavy ion composition in plasmasphere, together with their relative roles and times scales in individual storm events. The Comprehensive Inner Magnetosphere-Ionosphere (CIMI) model is used to quantify the ring current heating rate via the Coulomb collisions, and then the Ionosphere-Plasmasphere-Electrodynamics (IPE) model is used to evaluate the impact on ionospheric plasma temperatures and resulting plasmaspheric composition. The model simulations are compared to multiple observations, such as RBSP, TWINS, ERG (ARASE), DMSP, and ISR.

MITC15 - Localized Neutral Temperature Responses to Magnetosphere-Ionosphere-Thermosphere Coupling- A Mechanism Study of Temperature Inversion Layer - by Haonan Wu

Status of First Author: Student IN poster competition PhD

Authors: Haonan Wu, Xian Lu, Gang Lu, Xinzhao Chu, Wenbin Wang, Liam Kilcommons, Delores Knipp, Boyi Wang, Toshi Nishimura

Abstract: The neutral temperature inversion layer (TIL) around 130lan is observed by the Fe Boltzmann lidar at McMurdo (78S, 166E), Antarctica, on 28 May 2011. None of the empirical models and default physics models capture the observation. We use TIEGCM driven by AMIE to explore the physical processes that lead to the TIL and the underlying MIT coupling. The aurora energy precipitation maps observed by DMSP/SSUSI are incorporated into TIEGCM since the empirical aurora maps in the model tend to underestimate both energy flux and mean energy. Using more realistic aurora maps, TIEGCM succeeded in reproducing the TIL. Additionally, we increased the electric variability in the aurora region, which significantly enhances the Joule heating in the lower E-region and leads to larger temperature enhancement and more obvious TIL. By diagnosing the thermodynamics equation, both the diabatic heating and adiabatic heating are found to be important in generating the TIL. The enhanced Joule heating induces strong vertical atmospheric expansion, which leads to strong adiabatic cooling above 140lan. The differential heating between 140lan and 200km leads to the TIL.

MITC16 - Simulating magnetosphere-ionosphere coupling via field-aligned current - by Astrid Maute

Status of First Author: Non-student PhD

Authors: A. Maute, G. Lu, A. Richmond, D. Knipp, Y. Shi

Abstract: Magnetosphere-ionosphere (MI) coupling is crucial in modeling the thermosphere-ionosphere (TI) response to geomagnetic activity. In general circulation models (GCMs) the MI coupling is frequently realized by specifying the ion convection and auroral particle precipitation patterns from, e.g., empirical models or assimilative models. Using assimilative models, such as the Assimilative Model of Ionospheric Electrodynamics (AMIE), has the advantage that the ion convection and auroral particle precipitation patterns are self-consistent and based on available observations. However, assimilating data can be time consuming and requires expert knowledge, and therefore it is so far not the standard way of MI coupling in GCMs. With the availability of AMPERE data, there is an increased interest of employing field-aligned currents (FAC) in GCMs to represent the MI coupling. The FAC from AMPERE captures interhemispheric differences in the MI coupling not represented by empirical ion convection models. However, since GCMs mostly employ prescribed high latitude ion convection patterns little is known about differences in the TI response to high latitude forcing by prescribed FACs. In this study, we will compare with the help of a simulated geomagnetic storm the different MI coupling methods, i.e., AMIE, empirical ion convection and AMPERE field-aligned current. We illustrate the sensitivity of the Joule heating and low latitude electric field with respect of the spatial distribution of the aurora and ion convection for the different cases. The influence of interhemispheric differences in the MI coupling on the middle and low latitude thermosphere-ionosphere system will be examined.

MITC17 - Impacts of binning methods on high-latitude electrodynamics: Static vs boundary-oriented binning - by Qingyu Zhu

Status of First Author: Student IN poster competition PhD

Authors: Qingyu Zhu, Yue Deng, Arthur Richmond, Astrid Maute, Yun-Ju Chen, Marc Hairston, Roderick Heelis, Liam Kilcommons, Delores Knipp, Robert Redmon, Elizabeth Mitchell

Abstract: An outstanding issue in general circulation model (GCM) studies is the underestimation of Joule heating, which could be associated with the binning methods in the development of the high-latitude electrodynamics drivers for GCMs. Traditionally, data are binned in fixed geomagnetic coordinates (i.e., through a static binning approach), which does not take the dynamic nature of the forcing into account and therefore may significantly smear out the high-latitude electrodynamics patterns. To avoid the smoothing issue, data can be binned according to some physically important boundaries in the high-latitude electrodynamics, i.e., through a boundary-oriented binning approach. In this study, we have investigated the sensitivity of high-latitude electrodynamics patterns to different binning methods by applying both static and boundary-oriented binning approaches to the electron precipitation and electric potential data from the Defense Meteorological Satellite Program (DMSP) dataset under moderately strong and dominant southward interplanetary magnetic field (IMF) conditions. As compared with the static binning results, it is found that the boundary-oriented binning approach can provide a more confined and more intense electron precipitation pattern. Besides, the electric potential and electric field increase near the convection reversal boundary (CRB), leading to a 7% enhancement of the cross-polar-cap potential. Moreover, both static and boundary-oriented binning patterns are used to drive Global Ionosphere and Thermosphere Model (GITM) to examine the impacts on Joule heating by using different binning patterns. As compared to the case where GITM is driven by static patterns, both localized and hemispherical-integrated Joule heating increases remarkably when GITM is driven by boundary-oriented patterns. Particularly, the hemispherical integrated Joule heating increases by 25%.

MITC18 - A case study of meso-scale electric fields and their effects on the I-T system - by Dogacan Ozturk

Status of First Author: Non-student PhD

Authors: Xing Meng, Olga Verkhoglyadova, Josh Semeter, Roger Varney, Ashton Reimer

Abstract: On March 2nd, 2017, the Poker Flat Incoherent Scatter Radar (PFISR) recorded high-resolution electric field measurements to assist ISINGLASS rocket campaign during moderate geomagnetic activity. The THEMIS-E spacecraft measured flow enhancements and magnetic field fluctuations at Earth's magnetotail. Correspondingly, measurements from a global network of ground-based radars showed short-lived, localized enhancements of ionospheric flows over Alaska. The PFISR measurements showed strong and dynamic electric field structures. These meso-scale structures (150-500 km, < 15 min.) play an important role in the coupling of Magnetosphere, Ionosphere, and Thermosphere systems at high-latitudes, transferring mass, momentum and energy. Global models help reveal the sources and effects of ionospheric perturbations on the Ionosphere-Thermosphere (I-T) system. However, these models are traditionally driven with empirical models, which can not resolve meso-scale structures spatially and temporally. We developed a novel method that combines local JSR electric field measurements with a global empirical model. The multi-scale electric potentials were then used to drive the Global Ionosphere Thermosphere Model (GITM) to investigate the effects of meso-scale drivers on the I-T system.

MITC19 - Optical Signatnre of Outer Radiation Belt Boundary - by Nithin Sivadas

Status of First Author: Student IN poster competition Masters

Authors: Nithin Sivadas, Josh Semeter, Toshi Nishimura

Abstract: The outer boundary of the outer radiation belt continuously loses energetic electrons (> 100 keV) into the ionosphere due to non-adiabatic pitch angle scattering processes. Unlike transient processes such as magnetic storms, they occur even during quiet periods as long as the magnetotail is stretched thin. Though previous studies have observed this type of precipitation, a quantitative estimate of their effects are lacking. Hence, we present detailed estimates of the conductivity enhancement, energy deposited, and optical signatures produced by the outer radiation belt boundary in the ionospheric D-region. The energetic electrons from the boundary form an arc that is ~2000 km long in longitude, and ~100 km wide in latitude, and has an energy flux > 1 mW/m² (for electrons > 30 keV). It has the potential to cause ozone depletion through NO_x production. The D-region Hall and Pedersen conductance due to the boundary is about 10 S and 0.7 S, which is about 25% and 5% of the total ionospheric conductance. The arc of energetic electrons moves equatorward slowly (-5 km/min) during the substorm growth phase, and borders the poleward shoulder of the diffuse aurora. They are also observed to be equatorward of the growth phase arc, and may have an effect on the current systems driving its brightening before onset.

MITC20 - Ionosphere modulation by Pc5 ULF waves and wave structure detected by PFISR - by Boyi Wang

Status of First Author: Non-student PhD

Authors: Boyi Wang, Yukitoshi Nishimura, Micheal Hartinger, Roger Varney

Abstract: ULF Pc5 mode waves (with a 40-600s period band) are very important electromagnetic waves in transporting particles and energy in the magnetospheric and ionospheric coupling system. However, how much Pc5 mode waves modulate the ionosphere and how they are structured spatially and propagate are still poorly understood. In this study, we investigate ionosphere modulation by Pc5 waves in the nightside and their structures by taking advantage of 3D observations by the Poker Flat Incoherent Scatter Radar (PFISR) radar. PFISR observations found that the ionosphere conductance is modulated by a substantial amount (-50%), giving -10% changes in the reflection coefficient. Inversion of the ionosphere density reveals the dominant population of electrons modulated by the Pc5 pulsations as ~10 keV electrons modulating by a factor of 2, while lower energy electrons are not modulated. The energy dependence allows to find the population that resonate with ULF waves. The multi-beam radar observations and auroral imaging also show that the waves propagate azimuthally at ~2 km/s away from midnight in the ionosphere, with $m \sim 50$. The propagation direction suggests that particle injections and subsequent drifts become the source of the nightside Pc5 waves.

MITC21 - Storm-Enhanced Density (SED) Formation and Structuring During the September 7, 2017 Geomagnetic Storm - by Zihan Wang

Status of First Author: Student IN poster competition Masters

Authors: Zihan Wang, Shasha Zou, Aaron Ridley

Abstract: Storm-Enhanced Density (SED) is the most prominent storm-time ionosphere high-density structure, and its formation and structuring mechanisms are still not well understood. Different mechanisms, including imbalance between the production and loss due to vertical lifting, have been proposed. In this study, we use the coupled BATSRUS-RCM model and the GITM model within the University of Michigan's Space Weather Modeling Framework (SWMF) to study the ionosphere-thermosphere responses during the September 7, 2017 storm. We quantify contributions of different formation mechanisms of the SED, and also study the physical processes structuring the SED, such as SED segmentation.

MITC22 - Effects of substorms on high-latitude upper thermospheric winds - by Ying Zou

Status of First Author: Non-student PhD

Authors: Ying Zou; Yukitoshi Nishimura; Larry Lyons; Mark Conde; Roger Varney; Vassilis Angelopoulos; Stephen Mende

Abstract: Substorms release a large amount of energy stored in the Earth magnetotail and this energy is deposited into the ionosphere and thermosphere. While the effects of substorms on the ionosphere (ionization, convection, currents, etc.) have been studied for decades, the effects on the thermosphere, particularly winds, are poorly investigated. Among the very limited available studies, seemingly contradicting conclusions have been presented: superposition analysis only indicates a weak perturbation of low tens of m/s on upper thermospheric winds, while case studies suggest significant changes of 200 *mis* or more. We systematically investigate the effects of substorms on upper thermospheric winds using a network of scanning Doppler imagers distributed over Alaska. The effects are studied at pre-midnight, midnight, and post-midnight sectors. We find that winds exhibit various spatial patterns, where they occur sometimes as a latitudinally broad enhancement, and sometimes as sheared zonal winds. For each pattern, wind perturbations commonly have a magnitude of 100-200 *mis*. The patterns are consistent with plasma convection when plasma measurements from PFISR are available, indicating that ion drag is an important force for accelerating winds. The results imply that a significant portion of the energy associated substorms is converted to kinetic energy of thermospheric neutrals thanks to a tight M-I-T coupling. The little impact reported previously may result from a superposition of different wind patterns.

POLAO1 - Measuring Ionospheric Variability Using HF Signals of Opportunity in the Antarctic - by Nathaniel Frissell

Status of First Author: Non-student PhD

Authors: N. A. Frissell, R. Melville, A. Stillinger, G. Jeffer, A. J. Gerrard, P. J. Erickson

Abstract: Sources of short-term ionospheric variability include sources from above, such as solar flares, geomagnetic storms, and particle precipitation, and sources from below, such as atmospheric gravity waves (AGWs) and traveling ionospheric disturbances (TIDs). This variability modulates signals that propagate through the ionospheric medium, including high frequency (HF, 3 to 30 MHz) radio signals that refract back to Earth. Signals of Opportunity, or radio signals from pre-existing transmitters such as government standards stations and amateur (ham) radio stations, provide a source of observables for sensing ionospheric variability. We designed a portable, solar-powered, Red Pitaya software defined radio (SDR)-based HF recording system and deployed it to McMurdo Station, Antarctica during the 2018-2019 field season. This system will simultaneously monitor 648 kHz-wide slices between 0.1 and 60 MHz and record the raw spectrum to disk using GNU Radio and the MIT Haystack Digital RF Software.

POLA02 - Comparison between 1-D and 4-D Ground Based Height Profiling Techniques to Resolve Altitude Variations of Neutral Winds in the Lower Thermosphere - by Kylee Branning

Status of First Author: Student IN poster competition PhD

Authors: Mark Conde

Abstract: Few techniques are available for measuring neutral winds at E-region altitudes, especially in the height range from approximately 120 to 150 km. In-situ probes are typically unable to remain aloft at these heights for more than a few hours, and remote sensing is largely ineffective in this range. Rocket-borne chemical release methods can provide absolute measurements for winds in this region; however, the cost of such experiments is too high for routine applications. The consequent scarcity of observations is a problem, because winds in this region are of scientific interest (due to the transition from atmospheric behavior to space-like behavior) and of operational interest (because of their impact on radio propagation and on higher altitudes where satellites orbit). One measurement technique in this region is to record Doppler spectra of the oxygen 558 nm and 630 nm emissions using an all-sky viewing Fabry-Perot interferometer (FPI). It is known that the characteristic energy of electron precipitation can change by many keV on time scales of minutes or less causing amorally excited 558 nm emission heights to vary both across the sky and over time. This behavior coupled with the strong altitude gradients of wind and temperature that are known from chemical releases to occur at these heights has been used previously to construct an altitude profile of wind. However, this technique only provides a one-dimensional view of the wind fields as an average over both the time period and the horizontal extent of the field of view. The horizontal spatial averaging requires a uniform wind field, whereas sampling a range of altitudes requires spatial and temporal variation in the characteristic energy of electron precipitation during that measurement period. For these reasons, the 1-D technique is limited. In order to better resolve the winds over a large region, it is possible to create a four-dimensional wind field using the Doppler spectra of the oxygen 558 nm and 630 nm emissions. This technique starts with a base-line initial wind field that is easily generated from the data as a very crude approximation. Using an evolutionary algorithm, repeated small perturbations are applied at a range of longitude, latitudes, altitudes, and times. The algorithm then determines a (signed) magnitude for this perturbation that will best improve goodness of fit. This method has shown to be more versatile than the one-dimensional technique as it can be used on any night that data are available. Examples and comparisons of both techniques will be presented.

POLA03 - UV Tomography in the Cusp - by Bruce Fritz

Status of First Author: Non-student PhD

Authors: Bruce Fritz, Ken Dymond, Stan Solomon, Larry Paxton, Ethan Miller, Marc Lessard

Abstract: The cusp is a highly structured, dynamic environment that is driven by a variety of energetic inputs. Data are presented from the Special Sensor Ultraviolet Limb Imager (SSULI) and the Special Sensor Ultraviolet Spectrographic Imager (SSUSI) on the Defense Meteorological Spacecraft Program (DMSP). Data are inverted using the Volume Emission Rate Tomography (VERT) method to show the vertical emission structure of the region. Particle precipitation measured by the DMSP spacecraft is used to drive the Global Airglow (GLOW) model for comparison to the tomographic reconstruction. Results are then compared to the Rocket Experiment for Neutral Upwelling (RENU) 2 that launched on 13 December 2015 and measured a weak upwelling event in the cusp.

POLA04 - High resolution Kelvin-Helmholtz Instabilities observed during the 2018 PMC Turbo flight - by Carl Kjellstrand

Status of First Author: Student IN poster competition PhD

Authors: David Fritts, Christopher Geach, Shaul Hanany, Glenn Jones, Bernd Kaifler, Natalie Kaifler, Michele Limon, Amber Miller, Jason Reimuller, Bifford Williams

Abstract: PMC Turbo was a balloon-borne experiment that observed gravity wave dynamics in Polar Mesospheric Clouds (PMCs) above the Arctic. The PMC Turbo payload included seven optical cameras and a Rayleigh backscatter lidar. It launched from Esrange, Sweden on July 8th 2018 and landed undamaged in western Nunavut, Canada on July 14th. PMCs form an often thin and bright layer at about 82 km altitude in which brightness fluctuations reveal small scale dynamics in the upper mesosphere in polar summer. The PMC Turbo mission was designed to explore the dynamics of gravity waves and the gravity wave breaking and shear instabilities accounting for turbulence, mixing, and gravity wave energy and momentum deposition via high-resolution imaging of the dynamics over the life cycles of multiple events. Due to the high viscosity in the upper mesosphere, PMC Turbo imaging captured spatial scales from gravity waves with wavelengths of roughly 10-100 km, instability dynamics at scales from about 1-10 km, and fine structure near the inner scale of turbulence at about 20 m. One important class of dynamics observed by the experiment was intense and complex Kelvin-Helmholtz instabilities (KHI). KHI can be induced at a large scale by GWs with near-inertial frequencies. In addition, smaller GWs can locally perturb sheared layers to create regions of KHI. PMC Turbo data contains examples of KHI that have been strongly modulated by gravity waves. The formation and subsequent turbulent dissipation of KHI is an important method of energy and momentum deposition by GWs. The PMC Turbo experiment observed complicated interactions between KHI billows which violently break into turbulence. The data was recorded with sufficient temporal and spatial resolution to compare with direct numerical simulations of KHI interactions. This poster will examine the large scale context and small scale dynamics of KHI observed by PMC Turbo.

POLAOS - The effect of sustained magnetic activity on Joule heating rates in the polar cap -
by Andrew Kiene

Status of First Author: Non-student PhD

Authors: A. Kiene, W. A. Bristow, M. G. Conde, and D. L. Hampton

Abstract: It has been thought that Joule heating near 250 km may lead to thermal expansion of the neutral atmosphere that results in anomalously high neutral densities in the polar cap, as reported by the CHAMP satellite and others. The combination of ion velocities from SuperDARN and neutral wind and temperature measurements from Scanning Doppler Imagers in the Antarctic can be used to produce estimates of ion temperatures and Joule heating rates in the polar cap. Preliminary work has shown that the smaller ion velocities, combined with weaker precipitation inside the polar cap, means that the neutrals are relatively unaffected by ion-neutral momentum coupling and that the neutral wind buoys the Joule heating rate when ion velocities are small and produces very little variability in the heating rates when compared with auroral regions. In this study, we examine several longer periods of sustained moderate geomagnetic activity and compare them with quiet periods of similar length in order to investigate the variability of Joule heating rates.

POLA06 - Characterizing unexpected slowing of the Cross Polar Jet over Alaska in the midnight sector - by Rajan Itani

Status of First Author: Student IN poster competition Masters

Authors: Rajan Itani, Mark Conde

Abstract: We have studied the auroral zone thermospheric winds in the midnight local time sector, using ground based optical Doppler spectroscopy of the 630 nm emission from atomic oxygen at around 240 km altitude. One of the most prominent recurring features seen in winds at these latitudes is the cross-polar jet emerging from the polar cap at local times around magnetic midnight. The standard view is that wind flows anti-sunward in the midnight sector, and spills equatorward over magnetic latitudes extending well below those of the auroral zone. The purpose of this study is to show that the existing view is too simplistic. At the magnetic latitudes of our observatory at Poker Flat, Alaska, (-65 degrees), the anti-sunward flow is frequently seen to stall without spilling further equatorward. This behavior is most prevalent during low solar activity at mid-winter, when the combination of pressure gradient established by solar heating and the ion drag are not enough to allow the jet to push through the background atmosphere on the night side. At higher latitudes, by contrast, the flow is relatively uniformly anti-sunward around magnetic midnight (as expected in the polar cap), even during quiet conditions. During periods of higher solar and magnetic activity, the cross polar jet does spill equatorward over Alaska in the midnight sector as expected. This is a very significant feature in the high latitude wind system where the observation appears inconsistent with the model behavior. So we want to study and characterize this unexpected feature.

POLA07 - Effects of Energetic Particle Precipitations on Thermospheric Nitric Oxide Cooling - by Cissi Lin

Status of First Author: Non-student PhD

Authors: Cissi Y. Lin, Yue Deng, Delores J. Knipp, Liam M. Kilcommons

Abstract: Satellite measurements have revealed significant enhancement of nitric oxide (NO) emission at 5.3- μm during shock-led interplanetary coronal mass ejection (!CME) events. The abnormally high enhancement of NO cooling during these events may contribute to the problem storms, during which model predictions of neutral density have great discrepancies. While it is well-known that particle precipitation is the primary mechanism for the NO emission enhancement at the polar region, the relative significance of ions, soft electrons, and keV-electrons is yet to be well determined. The goal of this study is to identify contribution of electron and ion (of each energy band) precipitations to the thennospheric NO cooling enhancement by using the Defense Meteorological Satellite Program (DMSP) spacecraft data. The observed energetic electrons and ions (0.1-30.2 keV) during -100 events in 2002-2010 are categorized according to the characteristics of!CME events and binned into geomagnetic grids to provide statistic distributions of the particle precipitation for the polar regions. The distributions are incorporated into the Global Ionosphere-Thermosphere Model. The results show that electrons play a dominant role to NO cooling, but ions are important as well and can contribute to up to 30% of NO cooling during gee-effective events. NO cooling enhancement during the events is proportional to the level of energy flux and is dominated by the energy flux of the electrons in the energy band of 1.4-6.5 keV. The global thermospheric and ionospheric responses show that both total electron content (TEC) and NO cooling enhance instantaneously at the source regions, but they have different lifetime and correlation with the particle precipitations. In general, the NO cooling and TEC enhancement with the precipitating energy has positive correlation. Cross c01Telation shows that paiticle precipitations have more direct and instantaneous impact on TEC enhancement while it takes a little longer for the atmosphere to be heated up for the cooling to proceed.

POLA08 - Overview of PFISR D-region capabilities - by Pablo Reyes

Status of First Author: Non-student PhD

Authors: P. Reyes, R. Varney, A. Reimer

Abstract: During precipitation events, Poker Flat Incoherent Scatter Radar (PFISR) can measure collisional incoherent scatter (IS) spectra sometimes even as low as 60km in altitude with very narrow spectral widths which allows for very precise line-of-sight (LOS) Doppler velocities (e.g. Nicolls et al 2010). In this work we review the type ofD-region measurements that are possible with PFISR and discuss new capabilities, e.g. high temporal resolution spectra. Finally, we propose standard data products to be routinely processed and shared with the scientific community.

POLA09 - New HIWIND Observational Results from 2018 Flight - by Qian Wu

Status of First Author: Non-student PhD

Authors: Qian Wu, Delores Knipp, Ingemar Haggstrom, Roger Varney, Robert Gillies, Geonhwa Jee, Young-Sil Kwak, Mike Greffen, Phil Erickson.

Abstract: HIWIND, the first balloon-borne Fabry-Perot interferometer (FPI), flew from Kiruna to western Canada from June 24 to 31, 2018. It observed thermospheric winds along the flight track for more than 5 days. During the flight, incoherent scatter radars (ISR) at Kiruna, Millstone Hill, Resolute, and Poker Flat made simultaneous observations of ion drift and other ionospheric parameters as HIWIND passing nearby. This is the first time HIWIND made daytime thermospheric wind observations inside the polar cap during the summer season. In the past, there is a huge gap in the thermospheric wind coverage in the summer polar cap due to the long daylight hours. That has left a large uncertainty in our understanding of the ion-neutral interaction in the high latitudes. Model results were not validated. Daytime observation thermospheric wind in the polar cap is urgently needed. HIWIND filled this critical data gap. In this presentation, we will show the new observational results from the HIWIND instrument and ISRs and discuss what the results reveal about the polar cap thermospheric and ionospheric dynamics during the **summer season**.

C, ,,

Akbari, Hassan	16,17	Lamarche, Leslie	4
Albarran, Robert	24	Lejosne, Selene	27
		LeMay, Meghan	14
Bernstein, Valerie	1	Liang, Jun	28
Blandin, Matthew	25	Liao, Chi-Ting	11,12
Branning, Kylee	34	Lin, Cissi	37
Breitsch, Brian	12,13	Liu, Lei	22
		Longley, William	13
Chakraborty, Shibaji	19	Lopez, Aurora	8
Chatterjee, Kausik	24,25		
Chen, Shih-Ping	2	Malins, Joseph	14
Chen, Yun-Ju	25,26	Maruyama, Naomi	29
Chen, ZhiQing	18	Maute, Astrid	30
Coppeans, Thomas	2	Mehta, Piyush	18
		Moser, Crystal	23
De La Jara, Cesar	12	Mrak, Sebastijan	8
Debchoudhury, Shantaqnaab	19		
Dewan, Himani	14	Oborn, Benjamin	15
Diaz Pena, Joaquin	26	Ozturk, Dogacan	31
Elliott, John	3	Palo, Scott	17,18
		Ponder, Brandon	20
Forsythe, Victoriya	17		
Frissell, Nathaniel	34	Ren, Jiaen	5
Fritz, Bruce	35	Reyes, Pablo	37
		Rojas Villalba, Enrique	9
Goodwin, Lindsay	3		
		Shahbazi, Anahita	9,10
Hoffman, Alex	15,16	Shi, Vining	29
Hogan, Benjamin	27	Sivadas, Nithin	32
Hong, Cheng Ming	1,2	Smith, Dallin	7
Horton, Wendell	3	Smith, Jonathon	4
Irvin, Robert	4	Thomas, Leonard	23
Itani, Rajan	36		
		Vaggu, Pralay Raj	6,7
Jonah, Olusegun	22		
Joshi, Dev	10	Wang, Boyi	32
Joshi, Pratik	21	Wang, Jack	10
		Wang, Zihan	33
Ke, Kai-Jun	15	Weimer, Daniel	20
Kiene, Andrew	36	Wu, Haonan	30

Kilcommons, Liam	23, 24	Wu, Qian	38
Kjellstrand, Carl	35	Wu, Qian	38
Kumar, Narender	16		
Kunduri, Bharat	26, 27		